Heavy Lifters Design Team

Virginia Polytechnic Institute and State University
Free-Weight Final Report Spring 2007

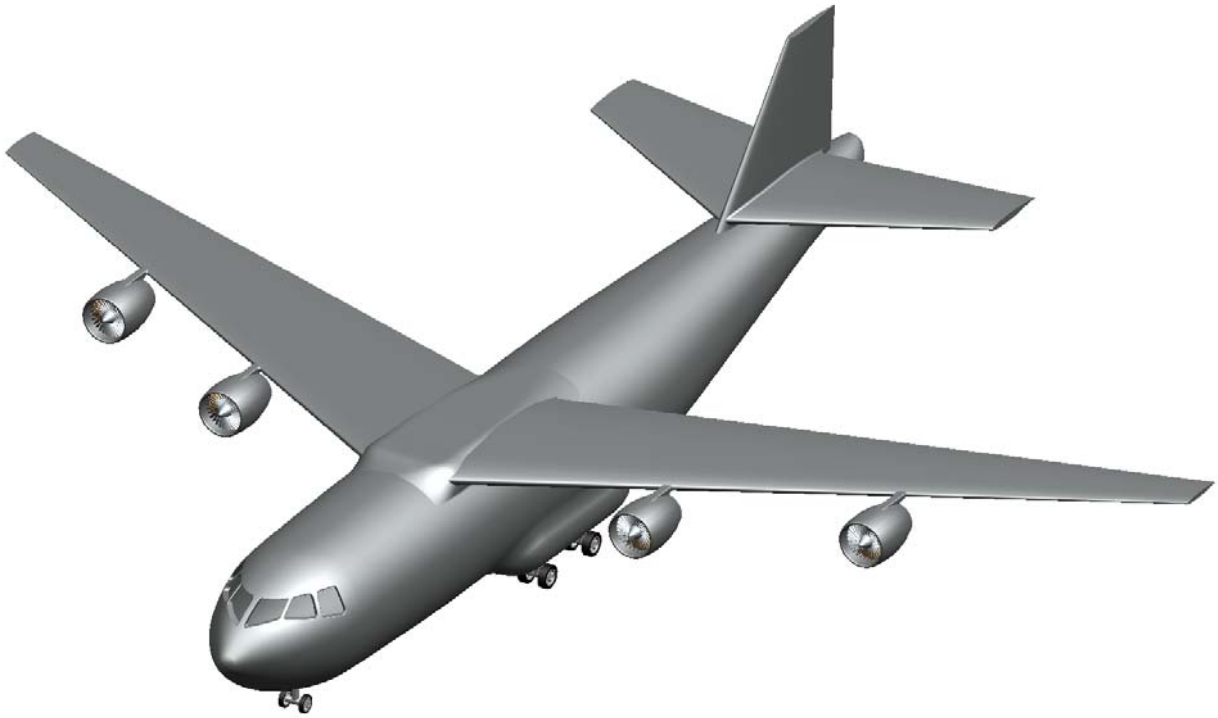

The Heavy Lifters

Leslie Mehl ***AIAA # 281854***	**Jonothan Rivers** ***AIAA # 281891***
Daniel Opipare ***AIAA #275371***	**Anne Parsons** ***AIAA # 281833***
Dzejna Mujezinovic ***AIAA # 235624***	**Kenneth Min** ***AIAA # 281693***
Kyle Nam ***AIAA # 278624***	**Michael Mangan** ***AIAA # 274249***
Zachary Cates ***AIAA # 281844***	**Jonathan Hall** ***AIAA # 282344***

Executive Summary

In contemporary warfare, there is a constant need for innovative technologies and designs for defense vehicles of all types. The modern battlefield is in an infinitely dynamic state, implying the necessity for military vehicles to operate in conditions never required of them in the past. In particular, a new breed of aircraft is needed that is capable of traversing the globe, carrying large cargo loads, and taking off and landing in far less than perfect conditions. Thus is the basis for the design of the *Free-Weight.*

Designed by the Heavy Lifters Design Team of Virginia Polytechnic Institute and State University, the *Free-Weight* meets all of the complex needs of the modern United States Military short take-off and landing, heavy cargo aircraft. It provides the ability to travel at least 500 nautical miles at speeds of at least Mach 0.8. During this travel, it is capable of carrying a payload weight of at least 60,000 pounds. These are just a few of the capabilities that the *Free-Weight* has to offer. In accordance with the AIAA Request for Proposal for 2006-2007, the additional capabilities of the *Free-Weight* are specific to the requirements of this RFP.

The Heavy Lifter Design team has created a concept to answer the AIAA design competition requirements. These requirements encompass two different mission scenarios for a transport vehicle capable of making short takeoff and landings in combat areas. The specific RFP requirements are stated in the following pages of this report.

Request for Proposal Requirements *As provided by the AIAA*

Transport Mission

- Payload
  - 25 tons with additional 5 tons of support equipment
  - Volume of dimension: 56 in. long, 128 in. wide, and 114 in. high
  - Additional 12 in. wide escape path around the vehicle
  - Center of gravity of the vehicle located 28 in longitudinally, 64 in laterally, and 48 in above the ground
- Aircraft structural design meets MIL Spec regulations for transport aircraft
- Crew
  - Flight crew: 2 (pilot and copilot)
  - Cabin crew: 1 (loadmaster)
- Warm-up and taxi at idle power for 8 minutes.
- Takeoff fuel allowance equal to the fuel consumed during 2 minutes of operation at max takeoff power.
- Balanced field takeoff length must not exceed 2,500 ft. at 95^{o}F at sea level.
- Cruise/climb to best cruise altitude
- Cruise at best cruise altitude and $M_{cruise} \geq 0.8$ for 500 nm less distance traveled during climb out
- Descend to 1000 ft for 100 nm at speed of Mach 0.6
- 5 minutes at three quarters take off power for landing if powered lift used
- If powered lift not required, use idle power
- Landing Zone
  - Blacktop (CBR=4 - 6)
  - Useful area of 3000 feet by 150 feet
  - 50 foot obstacles at 250 feet from either end of the runway
  - Balanced field length of 2500 feet
- 25 knot crosswind with a 5 knot tailwind component during landing
- Takeoff under combat rules, with mirrored mission segments for return and climb over a 50 foot obstacle from a standing start

Ferry Mission

- Payload
  - 10 tons of bulk cargo
  - density of 20 lb/ft^3 when properly packed
- Aircraft structural design meets MIL Spec regulations for transport aircraft
- Crew
  - Flight crew: 2 (pilot and copilot)
  - Cabin crew: 1 (loadmaster)
- Warm-up and taxi at idle power for 8 minutes
- Takeoff fuel allowance equal to fuel consumed during 2 minutes of operation at max takeoff power
- Balanced field takeoff length must not exceed 2,500 ft at 95^{o}F at sea level
- Cruise/climb to best cruise altitude
- Cruise at best cruise altitude and $M_{cruise} \geq 0.8$ for 3200 nm less distance traveled during climb out
- Aerial refueling permitted to achieve range
- Descend to sea level
- Normal approach to runway of 2500 ft or less
- 5 minutes at three quarters take off power for landing if using powered lift
- If powered lift not required, use idle power
- Balanced field length of 2000 feet
- Taxi in and park at gate using idle power for 10 minutes.
- Enough reserve fuel for a missed approach plus 150 nm diversion and 45 minute hold at 5,000 ft

The basic requirements for this aircraft state that it must be able to carry payload the dimensions and weight of a future deployable armored vehicle. The aircraft must be capable of short take-off and landings on an unimproved runway. Considerations must be made for the required aircraft range, ensuring that the craft can safely be operated in combat situations. The transport must also be able to reach speeds of at least Mach 0.8.

While all criteria mentioned in the RFP must be met, several stand out as driving factors of the design. The speed, payload size, range, and conditions at landing are of the most concern. The engine selection is based on factors such as the required Mach of 0.8, as well as the take off and landing distance requirements. The take off and landing requirements will also drive the aerodynamic design of the craft. Stability will be concerned with wind effects during landing. The cargo hold and loading ramp must be designed in order to accommodate the payload size and ease of use in combat conditions. Fuel considerations must be made in order to ensure the aircraft can meet the range requirements for different missions, especially factoring in the differing payload requirements of the missions. Landing gear will be chosen based upon the potential runway conditions. Special attention will also need to be paid to engine out scenarios.

Above all, the plane must be a cost effective solution for the United States Military personnel to complete the mission requirements safely. Provisions must also be made for crew comfort and ease of use. All of the preceding factors have culminated into the design of the *Free-Weight*, and are detailed in this technical report.

Table of Contents

I. Concept Evolution 11

I.1 Number of Engines 14
I.2 Number of Landing Gear 17
I.3 Performance Parameters 18

II. Mission Performance Analysis 19

II.1 Weight 19
II.2 Center of Gravity 20
II.3 FDAV Mission 21
II.4 Ferry Mission 23
II.5 Takeoff Distance Analysis 24
II.6 Landing Distance Analysis 26

III. Aerodynamics 27

III.1 Wing Planform 27
III.2 Airfoil Section 29
III.3 High Lift Devices 32
III.4 Drag 33
III.5 Powered Lift Configuration 35

IV. Stability 36

IV.1 Static Stability 36
IV.2 Dynamic Stability 36
IV.3 Trim to C_{Lmax} 37
IV.4 Crosswing Landing 40
IV.5 Engine Out 40

V. Propulsion and Powered Lift Systems 42

V.1 Powered Lift Systems 42
V.2 Propulsion 45
V.3 Engine Analysis 46
V.4 Starting and Electrical Systems 49
V.5 Auxiliary Power Unit 51

VI. Airframe Structures **52**

VI.1 Materials 52
VI.2 Loading 57
VI.3 Wing Structure 59
VI.4 Fuselage Structure 63
VI.5 Tail Structure 65

VII. Aircraft Systems and Avionics **66**

VII.1 Counter Measure Systems 66
VII.2 Navigation Equipment 67
VII.3 Communications 68
VII.4 Fire, Air, Icing Systems 71

VIII. Landing Gear Configuration **73**

VIII.1 Main Gear 74
VIII.2 Nose Landing Gear 75
VIII.2 Shocks 76

IV. Cost & Manufacturing **79**

IV. Summary **80**

Coefficients & Symbols **82**

References **84**

List of Figures

I. Concept Evolution

I.1 *Hefty Hauler* Design Concept 11
I.2 *Short Stop* Design Concept 13
I.3 Exhaust Spread Estimate over Flaps 16

II. Mission Performance Analysis

II.1 CG Location vs. Weight 21
II.2 FDAV Mission Profile 22
II.3 Ferry Mission Profile 24

III. Aerodynamics

III.1 Wing Planform (Half-Span) 28
III.2 Boeing Commercial Airplane Company airfoil J 30
III.3 Pressure Distribution over a BACJ Airfoil at 0 Angle of Attack and Mach 0.8 31
III.4 Lift Coefficient vs. Angle of Attack with High Lift Devices 33
III.5 BACJ Airfoil with Slat and Triple-Slotted Flaps Deployed for Landing 33
III.6 C_l vs. C_d for BACJ Airfoil 34
III.7 C_{D0} vs. α for BACJ Airfoil 35

IV. Stability

IV.1 Elevator Deflection Requirement vs. Trim Lift Coefficient During Landing 38

V. Propulsion and Powered Lift Systems

V.1 Triple-Slotted Flap System 43
V.2 Augmentor Flap System 43
V.3 An-72 with USB 44
V.4 Internally Blown Flap System 44
V.5 Engine Performance Parameters 49
V.6 Electrical Usage Schematic 50

VI. Airframe Structure

VI.1 External Material Usage on *Free-Weight* 56
VI.2 Internal Material Usage on *Free-Weight* 57
VI.3 V-n Diagram 58
VI.4 Elliptical Wing Loading 59
VI.5 Wing Loading for the Forward and Rear Spars 60
VI.6 Shear Force Diagram for the Forward and Rear Spars 60
VI.7 Bending Moment Diagram for the Forward and Rear Spars 60
VI.8 Minimum Cross Section Area Required for the Forward and Rear Spars 61
VI.9 3-D Wire Frame Wing Structure 62
VI.10 2-D Wire Frame Wing Structure 62

VII. Aircraft Systems and Avionics

VII.1 Interior Cockpit Layout (A) 68
VII.2 Interior Cockpit Layout (B) 69
VII.3 Control Panel Layout 70

VIII. Landing Gear Configuration

VIII.1 C-5 Galaxy 73
VIII.2 A400M 74

List of Tables

I. Concept Evolution

I.1 Initial Concept Decision Matrix 14
I.2 Engine Out Comparison 15
I.3 Engine Configuration Decision Matrix 16
I.4 Performance Analysis of Initial Concepts 18

II. Mission Performance Analysis

II.1 Aircraft Weight 19
II.2 Aircraft Weight Component Calculations 20
II.3 Takeoff Analysis 26
II.4 Landing Analysis 26

III. Aerodynamics

III.1 Wing Planform Parameters 29
III.2 High Lift Devices 32
III.3 High Lift Configurations 32
III.4 Calculated Drag Coefficients for Polar Drag 34

IV. Stability

IV.1 Static Stability Derivatives 36
IV.2 Dynamic Stability Data 37
IV.3 Flight Conditions for Stability and Control Evaluations 38
IV.4 Stability Derivatives 39
IV.5 Crosswind and Tailwind Required Maneuvering 40

V. Propulsion and Powered Lift Systems

V.1 Powered Lift Comparison 42
V.2 Engine Bypass Ratio Comparison 46
V.3 Mission Segment Analysis Based on 4-Engine Configuration 47
V.4 Fuel Consumption Comparison 48
V.5 APU Specifications 51

VI. Airframe Structure

VI.1 Material Characteristics 56
VI.2 V-n Diagram Corner Points 58
VI.3 Bulkhead Locations and Functions 63

VII. Aircraft Systems and Avionics

VIII. Landing Gear Configuration

VIII.1 Candidate Tire Specs: Main Gear 75
VIII.2 Candidate Tire Specs: Nose Gear 76
VIII.34 Energy Absorption Efficiency of Shock Absorbers 76
VIII.5 Landing Gear Weight Breakdown (% total weight) 77

I. Concept Evolution

A large period of time was devoted to the initial concepts by gathering ideas from current aircraft that have similar uses and capabilities as the requirements of set forth in the RFP. After further refinement, these initial concepts were later combined into a final design that would meet all of the necessary requirements. The *Free-Weight* is essentially a hybrid of two distinct initial design concepts. As the aircraft developed, specific traits of each of these designs were carried over into the final design of the *Free-Weight* to best meet the RFP conditions.

The first of the initial design concepts that the *Free-Weight* was based on was the *Hefty Hauler* design. The three-view of this design can be found in Figure I.1.

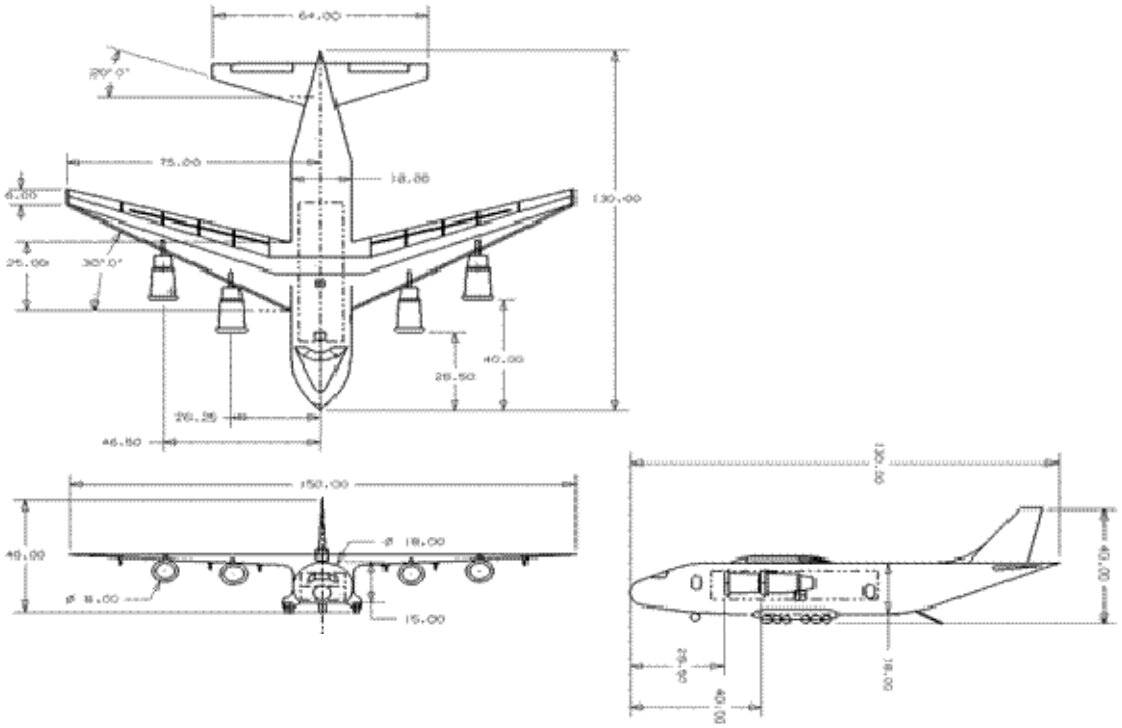

Figure I.1 "Hefty Hauler" Design Concept

The primary goal of this particular design is simplicity. It utilizes existing technology in order to provide ease of manufacturability, lightweight design, and to keep costs low. The design uses conventional designs for the tail, engine mounting system, and loading ramp for cargo. It incorporates a kneeling landing gear system, which is arranged in five sets of four wheels. This adds robustness to the design for the rough landing that this aircraft is likely to encounter and must be able to withstand, as well as making the loading and unloading of the cargo easier. It uses two turbofan engines to provide thrust and reduce weight expense, and an exotic flap system to provide high-lift capabilities. The *Free-Weight* borrowed some of these concepts from existing aircraft, which is explained in more detail later in the paper.

The other design that was incorporated into the final concept was the *Short Stop*. This aircraft has a slightly more complex design and utilizes more advanced technologies, but provides benefits that the *Hefty Hauler* does not. The *Short Stop* has a four engine design with a conventional tail configuration. It uses an externally blown flap system to provide higher lift coefficients for the short take-off and landing requirements on the aircraft. It utilizes a more complex loading configuration, using a half clamshell tail loading. This concept also employs existing technology to provide a certain degree of simplicity to the design and ease of manufacturability, as well as the safety and assurance of incorporating previously tested configurations. The final design concept was based in large part on this initial design. A three-view of this design can be found in Figure I.2.

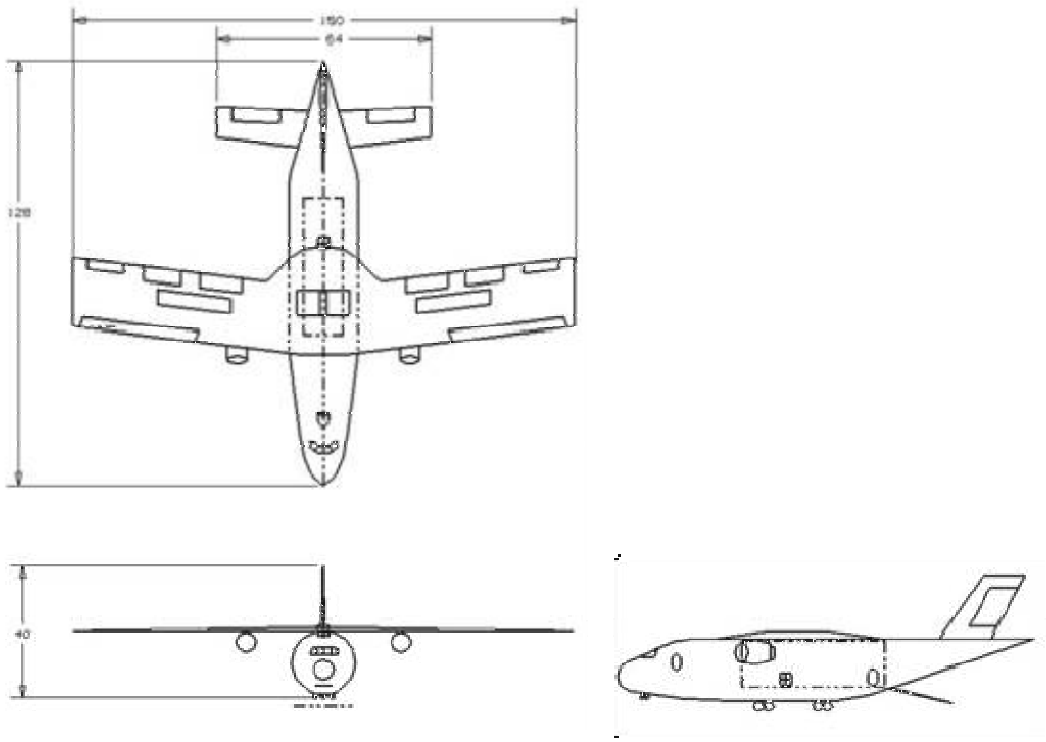

Figure I.2 "Short Stop" Design Concept

A large part of the decision-making process in the development of the *Free-Weight* was the use of a detailed decision matrix. Below is the initial concept decision matrix that was the basis of the choices in every area of the final design concept. It also provides a comparison of other comparator aircraft in a similar field in order to provide more detailed information about the particular design decisions that were made.

Table I.1 Initial Concept Decision Matrix

Weight	Criterion	An-70	Tu-330	C-17	*Short Stop*	*Hefty Hauler*
0.7	Manufacturing	8	9	9	8	10
0.9	Weight	9	8	1	8	9
0.8	Cost	10	8	1	7	9
1.0	Mission	5	10	8	10	9
1.0	Loading	10	10	10	10	10
1.0	Landing	7	10	4	8	10
0.5	Appearance	8	8	7	8	7
0.9	Maintenance	8	8	5	8	9
1.0	W/S	10	8	5	8	7
1.0	Size	5	5	1	10	10
0.7	Originality	10	6	8	8	6
0.7	Stability	8	8	10	10	9
	Total:	82.5	83.9	56.6	88.2	90.4

It is apparent from the technical drawings on the previous page and the concept decision matrix that distinct differences exist between the two concepts that need to be explored in further detail. The characteristics that most distinguish these two concepts from one another are the following:

- Number of engines
- Number of landing gear
- Performance Parameters

I.1 Number of engines

The most distinctive and noticeable difference between the two conceptual designs is the number of engines each design employs. The two concept aircraft, the *Hefty Hauler* and *Short Stop*, both utilize medium bypass ratio engines. Where there design differs is in the engine configuration, with *Short Stop* using four engines, and the *Hefty Hauler* only having two. For an externally blown flap system, the more flow over the flaps, the greater

the lift. This gives the four engine configuration a solid lead as far as being able to generate greater lift. To decide on the final engine configuration, the engine performance with an engine out was looked at as one of the deciding factors. The additional weight of the engines and supporting APUs was also considered. Table I.2 shows a comparison of the two different configurations in an engine out situation.

Table I.2 Engine Out Comparison

	Hefty Hauler	***Short Stop***
Max Thrust	126138	42046
Meets Cruise Requirements	Yes	Yes
Meets Takeoff Requirement	Yes	No

Heaft Hauler meets all requirements with an engine out. As the aircraft is designed to operate in combat conditions, and may take off under fire, this is a major advantage. Note that the chart above is before engine scaling, to give a balanced look at each configuration. Both configurations meet the FAA requirements for an aircraft power level based on the power required formula of $\frac{100n}{n-1}$%.

The major disadvantage of the four engine configuration is its 16,000 lb weight penalty when factoring in the weight of the additional engines, structure, and APUs. There is also a significant cost increase for the added hardware, engines, and APUs. Another design point was needed to make a decision on the concepts, so performance of the powered lift system was analyzed for takeoff and landing considerations.

With powered lift being a major factor in this aircrafts capability, the impact of different engine configurations must be analyzed. A prominent externally blown aircraft is the C-

17, an aircraft that utilizes a four engine configuration and has a lift coefficient greater than 5. The C_{Lmax} that was found to be required for landing of the *Free-Weight* was 3.8, with the C_L for takeoff being much closer to 3. Assuming a wing lift coefficient near 3, an increase of at least 1 must be gained through an EBF system. Four engines permit exhaust velocity to be spread out over a wider area of flaps than a two engine configuration, resulting in higher lift. Figure I.3 shows the area of the wing and flaps affected in a four engine design.

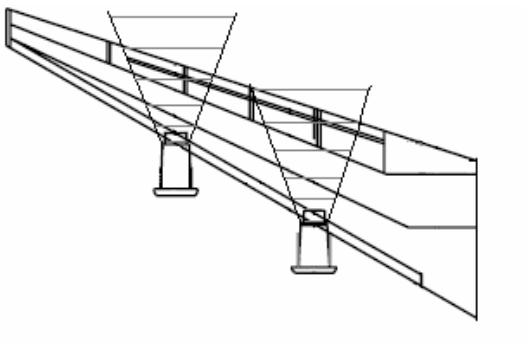

Figure I.3 Exhaust Spread Estimate over Flaps

In addition, during an engine out situation, the ability of the EBF system would be significantly decreased, for a two engine system, and less so for the four engine configuration. Table I.3 shows a decision matrix used to determine with engine configuration to use in the final design.

Table I.3 Engine Configuration Decision Matrix

	Two Engines	**Four Engines**
Weight (.7)	10	6
Cost (.6)	10	5
Maintenance (.4)	10	7
Engine Out Performance (.9)	4	10
Powered Lift Capability (1)	6	10
Totals	**26.6**	**29**

Further drag analysis of the completed airframe showed that at a cruise of Mach 0.8, two engines did not provide sufficient thrust at altitude to overcome the drag created. While this had not been a determining factor in the original configuration selection, it served to further verify the decision made. The four engine configuration is used on the final design, not only for its obvious advantages, but also its necessity at powering the aircraft to the required speeds.

I.2 Number of Landing gear

The *Hefty Hauler* is designed with landing gear in five sets of four wheels, which distribute the landing load, allowing the aircraft to land on the unimproved surface with a high CBR. This craft also incorporates a kneeling landing gear system to enable easier loading and unloading of cargo.

The *Short Stop* design uses a triple twin-wheel main landing gear located within pods, which allow the aircraft to have a lower profile. The fuselage, no longer having to contain the landing gear, can be shorter and wider, closer to the size of the FDAV required in the mission. Although the podding the landing gear will increase the drag of the aircraft, the new fuselage shape will lower the overall weight of the fuselage.

The final *Free-Weight* design merges aspects of both initial concepts, combining the main landing gear into side pods on the underside of the fuselage. In addition to decreasing the fuselage size required by podding the landing gear, the pods can also be used to store the aircraft APU and other systems. Podding the landing gear also allows

the landing gear to have a wider stance, lessening the likelihood of the aircraft tipping during landing.

I.3 Performance Parameters

Once the initial concepts for the design were chosen, preliminary analysis was done on the takeoff and landing distances. As can be seen in Table I.4, both concepts are capable of taking off and landing on a runway less than 2,000 ft long. Once the numbers were obtained, it was a matter of finding the best combination of thrust to weight ratio and C_{Lmax}, along with the optimum geometry.

Table I.4 Performance Analysis of Initial Concepts

Concepts	***Short Stop***	***Hefty Hauler***
Liftoff Velocity (ft/s)	140.5	137.7
Takeoff Time (sec)	11.05	20.67
Takeoff Distance (ft)	1265	1924.5
Landing Distance (ft)	1888.7	1845.4

These parameters and others factored in to the characteristics of the *Free-Weight* design, which is further described in the following report.

II. Mission Performance Analysis

The required mission performance is defined by the RFP and consists of two different missions, the first being that the aircraft must be able to transport a Future Deployable Armored Vehicle (FDAV) and the second being a transoceanic ferry mission. There is also a limit of 2500 ft for takeoff and landing balanced field lengths.

II.1 Weight

Given a restricted takeoff and landing distance, extra care was taken to minimize the weight of the aircraft. Certain decisions to minimize weight carried increased operating costs. One example is the use of low bypass ratio engines over heavier yet more fuel efficient medium bypass ratio engines. The final weight of the aircraft fully loaded with fuel comes in at just under 236,000 lb, and requires a C_L for takeoff of only 3.0. Table II.2 describes several weight statistics for the *Free-Weight*.

Table II.1 Aircraft Weight

Aircraft Weight (lbs)	
Empty Weight	116000
Maximum Weight	235614
Max Fuel Weight	62000

The max weight of the aircraft accommodates the FDAV mission payload with a full fuel load to complete the mission. The maximum weight of the aircraft itself is limited by the landing distance of the aircraft, which requires a landing C_L of 3.8, the maximum that can be provided by the EBF system. Table II.2 shows a detailed weight breakdown of the aircraft.

Table II.2 Aircraft Weight Component Calculations

Component	*Weight (lb)*	*CG from Nose (ft)*
Wing	21434	55
Fuselage	32000	57
Forward Engine Set w/ Structure	14360	47
Back Engine Set w/ Structure	14360	59
Horizontal Stabilizer	3300	113
Vertical Stabilizer	2060	115
APU	450	80
Loading Ramp and Lift	6000	80
Nose Gear	1000	20
Rear Boggies and Support Structure	5250	65
Radar and Front Avionics	150	5
Cockpit Avionics	2000	9
Electrical Conversion System	1950	70
Supplemental Electrical Systems	3000	50
Hydraulic System	2000	55
Air Conditioning System	2000	40
Crew Seating and Crew (3)	2000	12.5
Fuel	62000	51
Payload	60000	56
Total	235614	55.85

II.2 Center of Gravity

The center of gravity was a focal point of design for this aircraft. Due to the fact that the aircraft must fly with a 30-ton payload and a full fuel load in the beginning of the mission, and no payload with a near empty fuel tank, the CG must be placed carefully to ensure stability throughout the mission. It was determined that the CG should shift no more than 15% of the MAC, or 2.55ft. After finalizing the wing position, the CG was slightly ahead of the center of lift for stability, and directly over the CG of the payload itself when fully loaded. Figure II.1 shows the amount of CG travel at different segments of the mission.

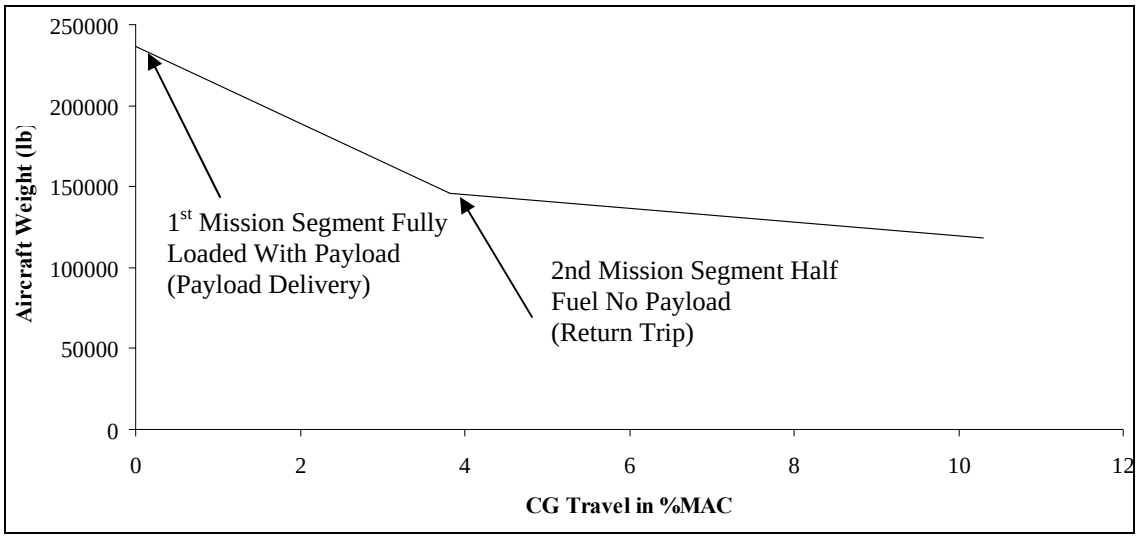

Figure II.1 CG Location vs. Weight

The forward and aft limits of the CG travel are shown as the mission progresses. The final CG for the loaded aircraft is 55.85 ft with the CG for the no payload landing configuration being 57.60 ft. The position of the wing and its effects on stability can be found in the *Stability* section.

II.3 FDAV Mission

The primary mission is the transportation of a total payload of 60,000 lbs and consists of thirteen segments, which can be dichotomized into the inbound and outbound portions, with one mirroring the other, and a payload drop-off in between the two. The first, as well as last, six segments of the mission are as follows. First, the aircraft must warm-up and taxi at idle power for 8 minutes. It must then take off at sea level in a temperature of 95°F with a balanced field length not exceeding 2,500 ft. The fuel allowance for takeoff is equal to the fuel consumed during two minutes of operation at maximum takeoff power. The aircraft must then climb to best cruise altitude and cruise for 500 nm at a velocity of at least Mach 0.8, less the distance traveled during climb out. Then it must

descend to 1,000 ft for 100 nm at Mach 0.6, and land while not exceeding a balanced field length of 2,500 ft. Five minutes at three quarters takeoff power was allocated for landing since powered lift was used. Using the mission program available from the university, the total range of the mission was 1200 nm, minus takeoff and landing. The total fuel required was found to be 62000 lbs, which allows for 887 lbs of trapped fuel. The details of the mission profile can be seen in Figure II.2.

The Free Weight, FDAV MIssion

PAYLOAD (0-5) = 60,000 lbs
PAYLOAD (7-12) = 0 lbs

TOGW = 236,000 lb
TOTAL FUEL = 62,000 lb

TAKEOFF DISTANCE (1) = 2213 ft
BALANCED FIELD LENGTH (1) = 2488.6 ft
TAKEOFF TIME (1) = 17.2 sec

Landing Distance (5) = 2477.6 ft

TAKEOFF DISTANCE (8) = 1194.4 ft
BALANCED FIELD LENGTH (8) = 1308 ft
TAKEOFF TIME (8) = 13.6 sec

Landing Distance (12) = 1719.1 ft

MISSION SEGMENT	SPEED (M)	ALT (ft)	L/D	TIME (min)	FUEL (lb)	DIST (nm)
0. WARM-UP, TAXI	----	SL	----	8	1844	----
1. TAKEOFF	0.23	SL	4	2	2498	----
2. CLIMB TO CRUISE ALT	0.7	-----	7	4.3	3749	37
3. CRUISE	0.8	35,000	16.5	60.2	11087	463
4. DESCENT TO 1000 FT	0.6	1,000	----	16.3	6647	100
5. LANDING	----	SL	4	5	5845	----
6. DROP OFF PAYLOAD	----	SL	----	----	----	----
7. WARM-UP, TAXI	----	SL	----	8	1936	----
8. TAKEOFF	0.23	SL	4	2	3223	----
9. CLIMB TO CRUISE ALT	0.7	----	7	2.4	2154	20
10. CRUISE	0.8	35,000	12	62.5	9842	480
11. DESCENT TO 1000 FT	0.6	1,000	----	16.2	6443	100
12. LANDING	----	SL	4	5	5845	----
TOTAL	**----**	**----**	**----**	**192**	**61113**	**1200**

Figure II.2 FDAV Mission Profile

II.4 Ferry Mission

The secondary mission consists of a maximum of fifteen segments with a payload of 20,000 lbs. For the ferry mission, the aircraft must first warm-up and taxi for 8 minutes. It must then takeoff with a maximum balanced field length of 2,500 ft in 95°F temperature at sea level. Then it must climb to best cruise altitude and cruise for 3,200 nm at a Mach of at least 0.8, followed by the descent to sea level for landing. Another requirement is that there must be enough reserve fuel to accommodate a missed approach plus a 150 nm diversion and hold at 5,000 ft for 45 minutes of loiter time. The landing requirement states that the aircraft must not exceed a balanced field length of 2,500 ft. Something to note is that since the fuel requirement was based on the FDAV mission, there was not sufficient fuel to accomplish the ferry mission. Thus, one aerial refueling is required for 40,000 lb of fuel, 2500 nm into the mission. This allows for 906 lb of trapped fuel. The refueling will be performed at the cruise altitude at a velocity of Mach 0.43, or 250 knots. The refueling will occur over 50 nm and last approximately 10 minutes. The details of the mission profile can be seen in Figure II.3. For both missions, the fuel flow was multiplied by 1.05 to account for any inefficiencies.

The Free Weight, Ferry Mission

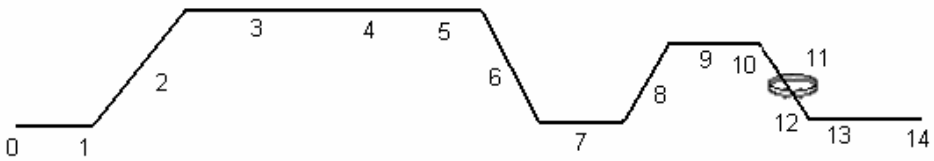

PAYLOAD = 20,000 lb	TOGW = 196,000 lb INTERNAL FUEL = 62,000 lb AERIAL REFUELING = 40,000 lb
TAKEOFF DISTANCE = 1711.8 ft BALANCED FIELD LENGTH = 1916.4 ft TAKEOFF TIME = 13.6 sec	LANDING DISTANCE (7) = 2175.2 ft LANDING DISTANCE (13) = 1867.9 ft

MISSION SEGMENT	SPEED (M)	ALT (ft)	L/D	TIME (min)	FUEL (lb)	DIST (nm)
0. Warm-up, Taxi	----	SL	----	8	1844	----
1. Takeoff	0.2	SL	4	2	2498	----
2. Climb	0.7	----	6	3.5	3029	29
3. Cruise	0.8	35,000	16	322	53315	2471
4. Aerial Refueling	0.43	35,000	18	10	943	50
5. Cruise	0.8	35,000	16	84.5	13229	650
6. Descend For Landing	0.6	----	----	17	----	----
7. Missed Approach	0.2	SL	4	2	6394	----
8. Climb	0.5	----	6	2	997	7
9. Divert	0.41	20,000	18	26	3339	143
10. Descend	0.4	----	----	7	----	----
11. Loiter	0.3	5,000	16	45	8074	----
12. Descend for Landing	0.3	----	----	2	----	----
13. Land	0.2	SL	4	2	5091	----
14. Taxi in, Park	----	SL	----	10	2341	----
TOTAL	**----**	**----**	**----**	**543**	**101094**	**3350**

Figure II.3 Ferry Mission Profile

II.5 Takeoff Distance Analysis

One of the design requirements as indicated in the RFP is the balanced field length. Since this competition is for the design of a short take-off and landing aircraft, it was one of the key mission drivers. The RFP also stipulates the air condition from which the aircraft must be able to takeoff, requiring the design to meet the balanced field length on a 95^{o}F day at sea level. This “hot day” atmospheric requirement reduces the air density to

0.00222265 sl/ft^3, which increases the takeoff distance when compared to takeoff at standard conditions. Another constraint is that the aircraft must be able to take off on a runway with a California Bearing Ratio between 4 and 6. This corresponds to a ground rolling friction coefficient somewhere between 0.03 and 0.1 [Ref 26]. The maximum value of 0.1 was used to account for worst case conditions. To determine the liftoff velocity, a stall margin of 1.2 was used.

The takeoff distance calculations were determined using the Krenkel and Salzman method [Ref 19] for a jet-propelled conventional and vectored thrust STOL aircraft. A few modifications were made to the method, mainly the addition a rotation phase and balanced field calculations. For the calculations, a rotation time of three seconds was used to reach optimum takeoff lift coefficient. Also, although engine failure was not required for takeoff analysis, one engine inoperative (OEI) was assumed in calculating the balanced field length to clear the 50 ft obstacle.

The Krenkel and Salzman method calls for the analysis of the takeoff run in two phases, the ground run and the climb run. In the ground run and the rotation phase, a nonlinear ordinary differential equation, as a function of the horizontal velocity, must be solved, and in the climb run, a system consisting of two nonlinear ordinary differential equations, as functions of the horizontal and vertical velocities, must be solved simultaneously. To determine the balanced field length, an iterative method was implemented until the takeoff and braking distances converged. The values for takeoff are shown in Table II.3.

Table II.3 Takeoff Analysis

Mission	FDAV (1)	FDAV (8)	Ferry
Weight (lb)	236,000	142,394	196,000
C_{Lmax}	3.8	3.8	3.8
C_{Lclimb}	3.0	3.0	3.0
Liftoff Velocity(ft/s)	229.9	224.1	224.5
Normal Takeoff Time (sec)	17.2	9.5	13.6
Normal Takeoff Dist (ft)	**2213**	**1194.4**	**1711.8**
Critical Velocity (ft/s)	135.2	73.7	112.1
Critical Dist (ft)	609.4	100.3	334.9
OEI Takeoff Time (sec)	19.1	10.8	15.2
Balanced Field Length (ft)	**2488.6**	**1308**	**1916.4**

II.6 Landing Analysis

Landing calculations were done using the method outlined in Raymer [Ref 25] which divides the landing into four sections: approach, flare, free roll, and braking distances. A stall margin of 1.2 was used for the approach velocity and 1.1 for the touchdown velocity. The obstacle height that needed to be cleared was 50 ft. Also, to meet the landing distance requirement, a total of 5,000 lb of reverse thrust, which could be obtained without the use of extra devices, was used during the breaking section. Table II.4 shows the landing calculations for the aircraft.

Table II.4 Landing Analysis

Mission	FDAV (5)	FDAV(12)	Ferry (7)	Ferry (13)
Weight (lb)	204,330	114,887	172,948	134,906
Approach Velocity (ft/s)	177.5	135.6	164	146.1
Touchdown Velocity (ft/s)	162.7	124.3	150.3	133.9
Vertical Touchdown Velocity (ft/s)	20.8	29.5	23.1	26.8
Approach Angle (deg)	7.4	13.7	8.8	11.54
Total Landing Distance (ft)	**2477.6**	**1719.1**	**2175.2**	**1867.9**

III. Aerodynamics

The RFP calls for long range cruise capability for each mission with a combat radius of 500 and 3,000 nautical miles respectively. To achieve the extremely short take-off and landing distances required, the aircraft must have the ability to fly at low speeds while remaining stable, and needs to cruise efficiently at Mach 0.8. The ability to operate efficiently for both low speeds at low altitude and high speed at high altitudes results in a well rounded cost effective design by reducing the need for other components to overcome any aerodynamic shortcomings.

III.1 Wing Planform

The design of the wing planform determines the majority of the aircraft's performance characteristics. In order to lift the large weight of the aircraft, the wing area needs to be considerably large. Based on preliminary sizing, the wing used on the Antonov AN70 was examined closely. The design follows the AN70's general shape and geometry. It was found that the area had to be increased from the AN70 baseline to provide enough lift for a smaller aircraft to achieve the performance characteristics defined by the RFP. To create a wing that operates efficiently at high speeds, in the near transonic region, the wing is swept to effectively reduce drag and delay shock formation at the cruise Mach of 0.8. The aspect ratio of the wing is high to maximize the lift to drag ratio. In order to have a high aspect ratio, the wing has a large span. For the design, the span was set to the allowable landing zone width of 150 feet. Elliptical wing loading is utilized in order to help maximize the lift to drag ratio. The wing planform is designed to be tapered to

produce a more elliptical lift distribution. The wing taper also allows for the wing structure to be lighter toward the wing tip. Research of similar aircraft showed the usefulness of a low to mild swept wing design with a moderate to large span resulting in a high aspect ratio trapezoidal wing. The design concept has to takeoff and land in shorter distances than many similar current aircraft. The wing is designed to be proportionally larger on a slightly smaller airframe to achieve the performance parameters needed for the RFP requirements. Wing planform is designed for high altitude, high speed operation with mild sweep to maintain maneuverability during takeoff and landing at low speeds. Historically, the most efficient design is a low sweep tapered trapezoidal wing. The conceptual design's semi-span wing planform can be seen in Figure III.1.

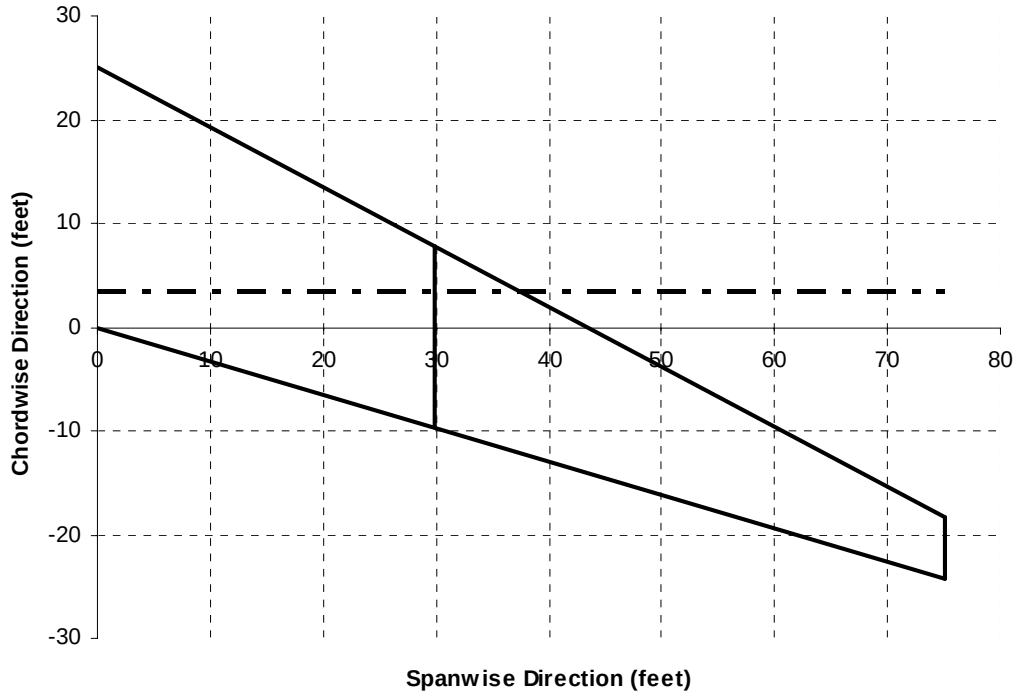

Figure III.1 Wing Planform (Half-Span)

Table III.1 shows the dimensions of the wing planform parameters.

Table III.1 Wing Planform Parameters

Root Chord (ft)	25.00
Tip Chord (ft)	6.00
Span (ft)	150.00
LE Sweep deg	30.00
Area (ft)	2325.00
Taper (tip/root)	0.24
Aspect Ratio	9.68
Mean Aerodynamic Chord (ft)	17.44
Y bar for Mean Aerodynamic Chord (ft)	29.84
Mean Aerodynamic Chord dist. From LE (ft)	17.23
Mean Aerodynamic Center from LE (ft)	21.59
W/S (max-with fuel)	103

III.2 Airfoil Section

The airfoil for the aircraft must have a high lift to drag ratio and a moderate lift coefficient at low angles of attack for cruise. The main concern for cruising at Mach 0.8 is the drag increase and loss of lift in the transonic region due to the formation of a shock wave on the upper surface of the airfoil. The shockwave forms because the flow over the top of the airfoil can accelerate to supersonic speeds. The formation of the shockwave creates a dramatic increase in pressure across the shock, causing loss of lift and a change in the boundary layer thickness which can result in flow separation. The Mach number in which the drag increase is due to the presence of a shockwave is referred to as the drag divergence Mach number. The shockwave formation can be delayed by using an airfoil which has laminar flow spread over a large portion of the upper surface, allowing for high lift characteristics while reducing the wave drag caused by formation of shocks. To acquire these characteristics, a supercritical airfoil was chosen. The airfoil used on the

Free-Weight is a Boeing Commercial Airplane Company airfoil, J model. The airfoil profile can be seen in Figure III.2.

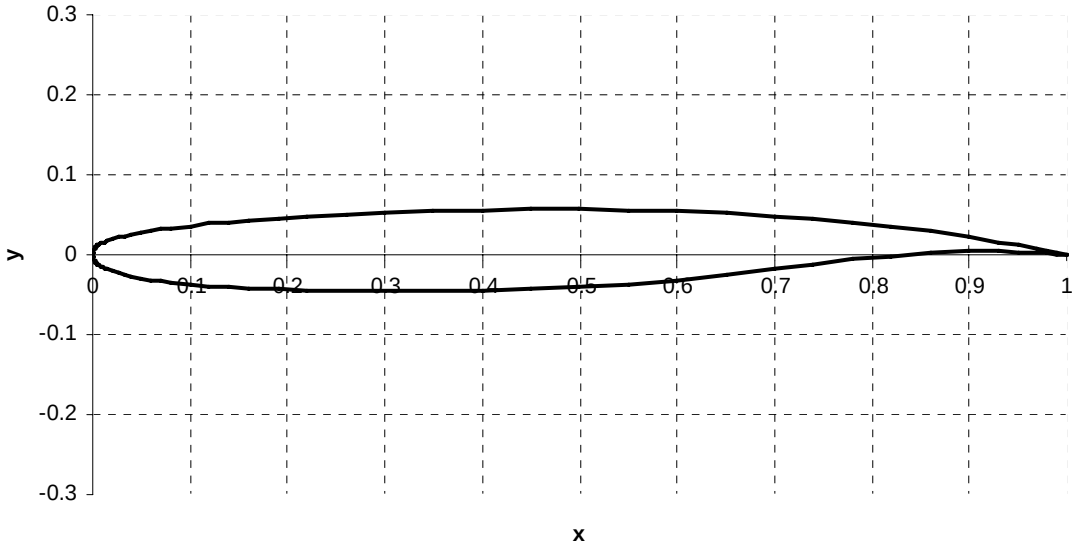

Figure III.2 Boeing Commercial Airplane Company airfoil J

This airfoil produces the lift coefficient needed for cruise at roughly -0.3 degrees angle of attack. A drag divergence Mach number occurs around Mach 0.82. This airfoil allows for cruise speeds of Mach 0.8 without a dramatic increase in drag due to shockwave formation. This configuration results in efficient cruise conditions, which cuts down on fuel consumption, weight, and cost. A transonic airfoil program, called Tsfoil2, was used to create a pressure distribution and velocity profile plot across the chord of the airfoil. Figure III.3 shows the airfoil pressure coefficient profile at zero degrees angle of attack.

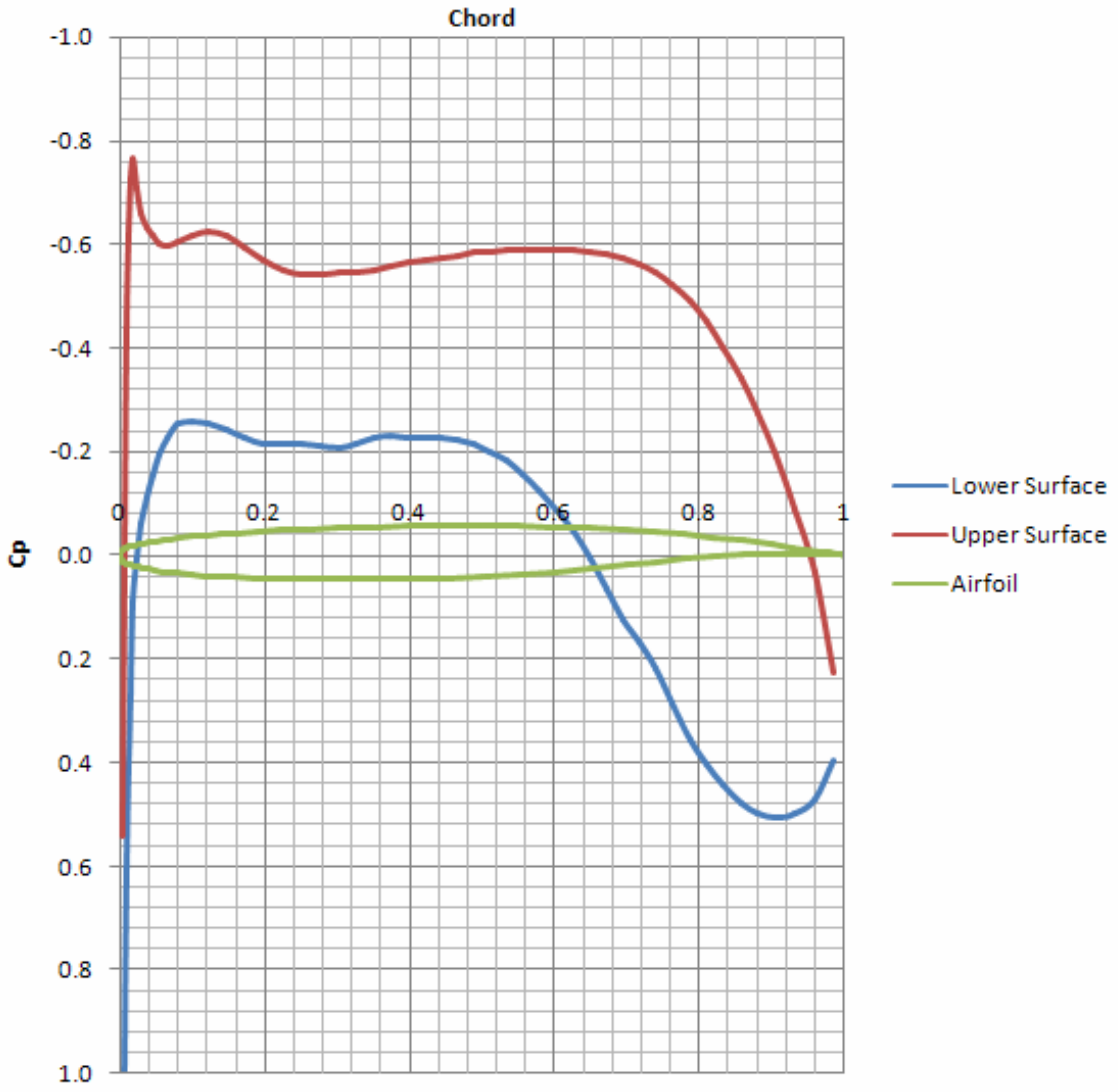

Figure III.3 Pressure Distribution over BACJ Airfoil at 0 Degrees Angle of Attack and Mach = 0.712

III.3 High Lift Devices

Using High Lift devices allows the *Free-Weight* to significantly increase its lift capability at low speeds. The ability to land and takeoff in short distances improves dramatically when the aircraft can maintain flight at lower speeds. The devices used can be found in the Table III.2.

Table III.2 High Lift Devices

High Lift Device Type	Location	Maximum Deflection	% Chord
Leading Edge Slat	Leading Edge	15º	10%
Triple-Slotted Flaps	Trailing Edge	68º	36%

The high lift flaps and slat will be used only for takeoff and landing where low speed flight is required. The leading edge slat effectively reduces the peak in pressure at the leading edge by creating camber. This raises the angle of attack at which C_{Lmax} is attainable and also lowers stall speed. The triple-slotted flap raises C_{Lmax} by creating a high cambered airfoil design for special configurations such as takeoff and landing where the benefits of a high lift cambered airfoil are desirable. The increased drag due to the flaps also helps to slow the aircraft's airspeed for short landing distances. Table III.3 shows the configurations used with the high lift system.

Table III.3 High Lift Configurations

Configuration	Leading edge Slat Deflection	Triple-Slotted Flap Deflection	C_{Lmax}
Cruise	0º	0º	1.954
Takeoff	15º	20º	2.619
Landing	15º	68 º	2.87646

NOTE: These C_{Lmax} numbers are conservative

The C_L needed for cruise at Mach 0.8 is no larger than 0.367. Calculating the lift coefficients for the high lift devices was accomplished with the use of [Ref 27]. A plot of

the lift coefficient with high lift devices vs. angle of attack for low speed flight can be found in Figure III.4.

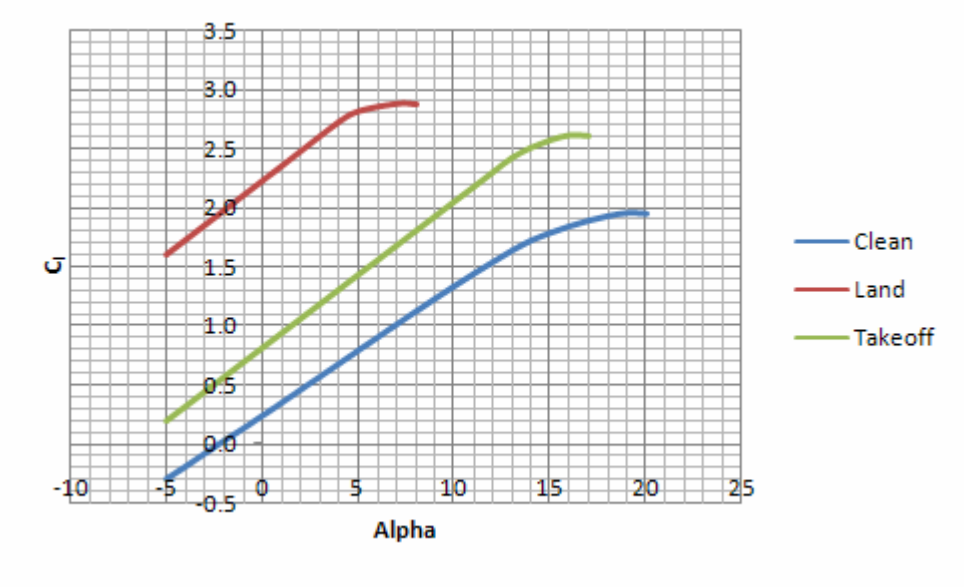

Figure III.4 Lift coefficient vs. angle of attack with high lift devices at Mach 0.2

Figure III.6 shows a conceptual drawing of the flap system for the final design concept.

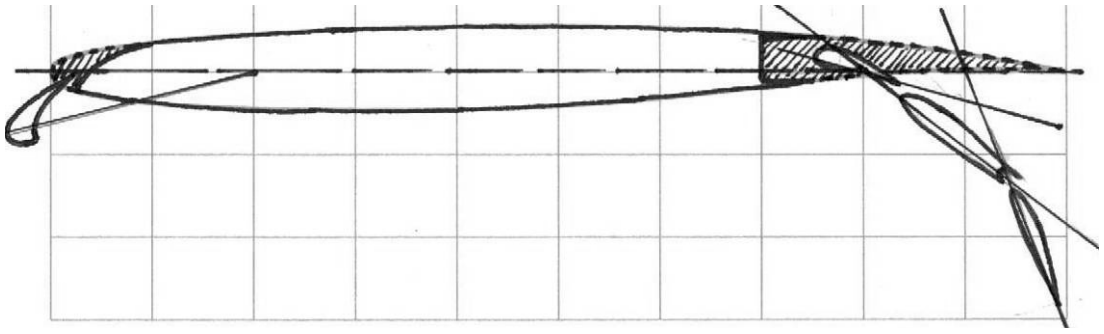

Figure III.5 BACJ Airfoil with Slat and Triple-Slotted Flaps Deployed for Landing

III.4 Drag

Estimates for polar drag were calculated using [Ref 27]. The calculations are based on the final design wetted area estimates for the wing ,fuselage, and other various components. Table III.4 displays some calculated results for takeoff and cruise conditions.

Table III.4 Calculated Drag Coefficients for Polar Drag

Configuration	Mach #	Altitude (ft)	C_{Do}
Takeoff	0.2	0	0.0195
Cruise	0.8	30,000	0.0182

A program called Xfoil 2.0 was used to estimate the airfoil characteristics in the subsonic region, which can be obtained by the University. The BACJ airfoil is expected to operate at angles of attack were the drag is very low when the airfoil is not using flaps. This low angle of attack operation will allow for decreased drag numbers across the aircrafts flight envelope. A plot of lift and drag coefficients can be found in Figure III.6.

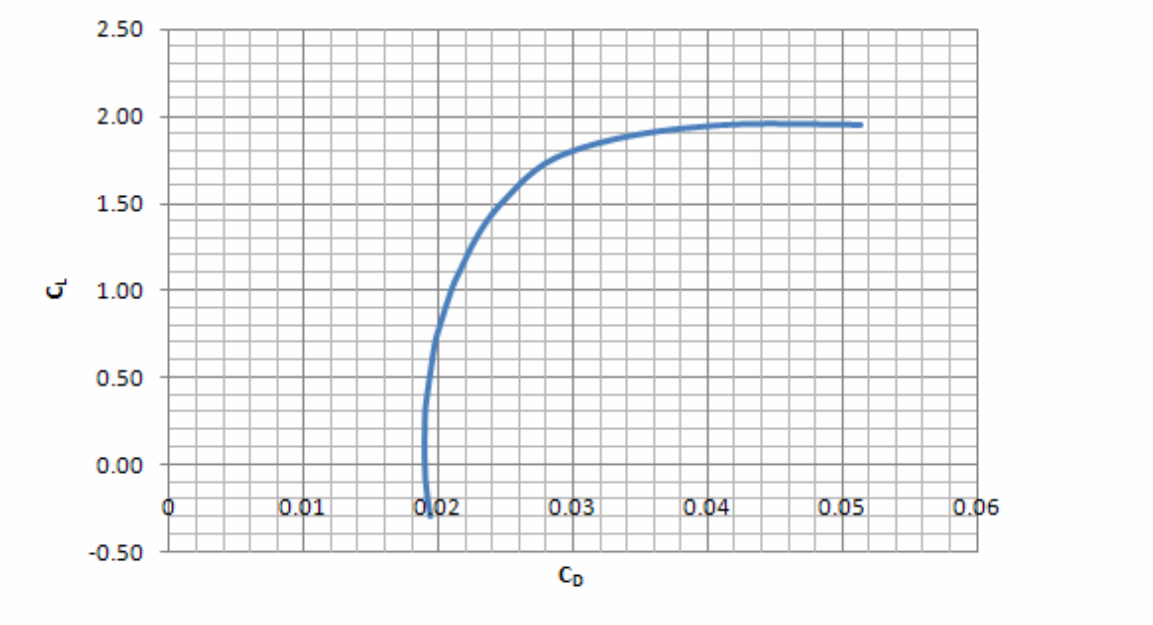

Figure III.6 C_l vs. C_d for BACJ Airfoil

The clear airfoil configuration demonstrates a similar effect on polar drag coefficient. Figure III.7 shows a plot of polar drag coefficient vs. angle of attack.

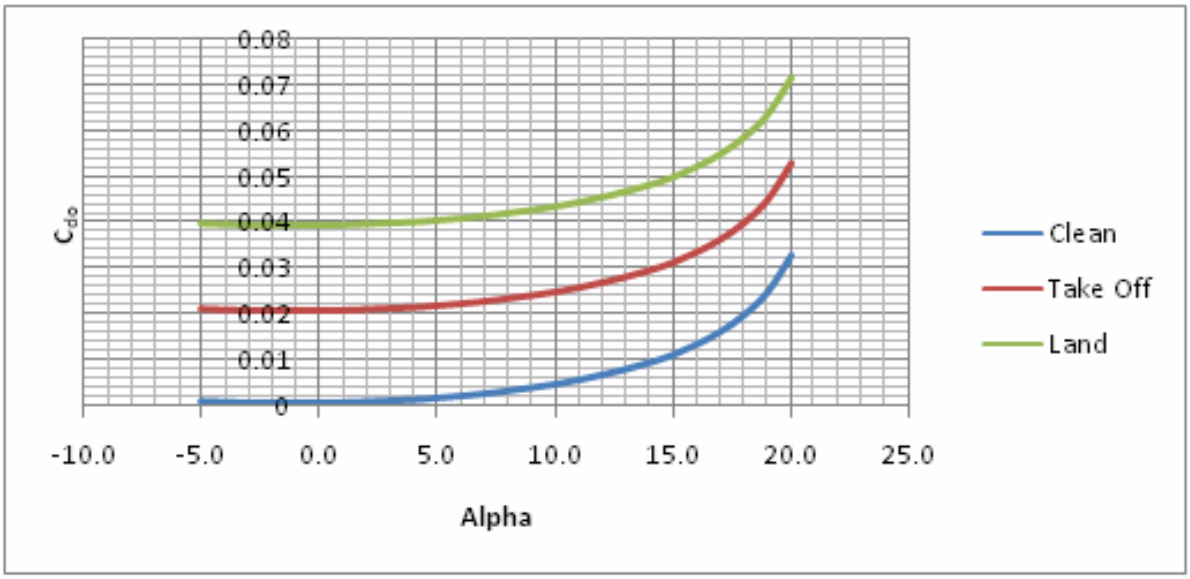

Figure III.7 C_{D0} vs. α for BACJ Airfoil

III.5 Powered Lift Configuration

The RFP calls for a landing distance of 2500 ft. Landing in such a short distance requires the aircraft to land at extremely low speeds. The ability to fly at low speeds requires a high maximum lift coefficient of nearly four. To get such a high lift coefficient, the wing has a complex externally blown flap configuration. The trailing edge of the wing contains a multi-slotted flap configuration that serves as the main source for increasing the lift coefficient over the entire angle of attack range during takeoff and landing. The flap configuration alone will not provide a sufficiently high lift coefficient. To reach the goal of a maximum lift coefficient of 3.8, the engine thrust is utilized to create an externally blown flap system.

IV. Stability

IV.1 Static Stability

The aircraft was designed to be inherently stable, with the center of gravity ahead of the neutral point. This results in a negative $C_{M\alpha}$. For directional stability, the yaw stiffness, $C_{n\beta}$, is positive and for rolling stability, $C_{l\beta}$, is negative. The values of the coefficients can be seen in Table IV.1.

Table IV.1 Static Stability Derivatives

$C_{M\alpha}$	-1.9
$C_{n\beta}$	0.044
$C_{l\beta}$	-0.017

IV.2 Dynamic Stability

The dynamic response was analyzed using the derivatives from the JKayVLM program, developed by Jacob Kay at Virginia Tech, and available from the university, and the methods used were from references 12, 31, and 37. The *Free-Weight* can be classified as a Class II or a Class III aircraft, so it was designed to meet the requirements for both. The responses analyzed were Phugoid, short period, and dutch roll. Since the FAR does not give specific values, the aircraft was designed to meet the requirements set by the military, as seen in [Ref 30]. As can be seen in Table IV.2, this design meets or exceeds all requirements.

Table IV.2 Dynamic Stability Data

	Level	Damping Ratio	MIL-STD Requirement	Frequency (rad/s)	MIL-STD Requirement
Short Period	1	0.467	0.35-1.3	4.064	0.87-7.2
	2		0.25-2.0		0.7-10.0
	3		> 0.15		> 0.6
Phugoid	1	0.043	> 0.04	0.0585	< 0.07
	2		> 0		
Dutch Roll	1	0.21	> 0.19	1.24	> 0.4
	2		> 0.02		> 0.4
	3		> 0		> 0.4

IV.3 Trim to C_{Lmax}

Due to the high lift required for landing, large pitching moments will occur. To verify the Heavy Lifter can trim at a C_{Lmax} of 3.8, as required during landing, while keeping its angle of attack below 15 degrees, so as not to scrape the ramp on landing, the following analysis was done. Using data from JkayVLM with a horizontal tail acting as a full elevator and landing at Mach 0.14 and a CG 57.5 ft from the front of the aircraft, a small program was written to calculate elevator deflections for various C_{Ltrim} values using a basic stability and control equation, Equation (1).

$$\begin{pmatrix} C_{L_\alpha} & C_{L_{de}} \\ C_{m_\alpha} & C_{m_{de}} \end{pmatrix} \begin{matrix} \alpha_{trim} \\ \delta e_{trim} \end{matrix} = \begin{matrix} C_{L_{trim}} \\ -C_{m_0} \end{matrix} \qquad (1)$$

CG travel will be very minimal, less than 3 feet, and does not cause the elevator deflection to reach values larger than -30 degrees. Figure IV.3 shows a plot of elevator deflection required for trim lift coefficients during landing. This shows that for a C_{Ltrim} equal to a C_{Lmax} of 3.8, the required elevator deflection is -18.42 degrees.

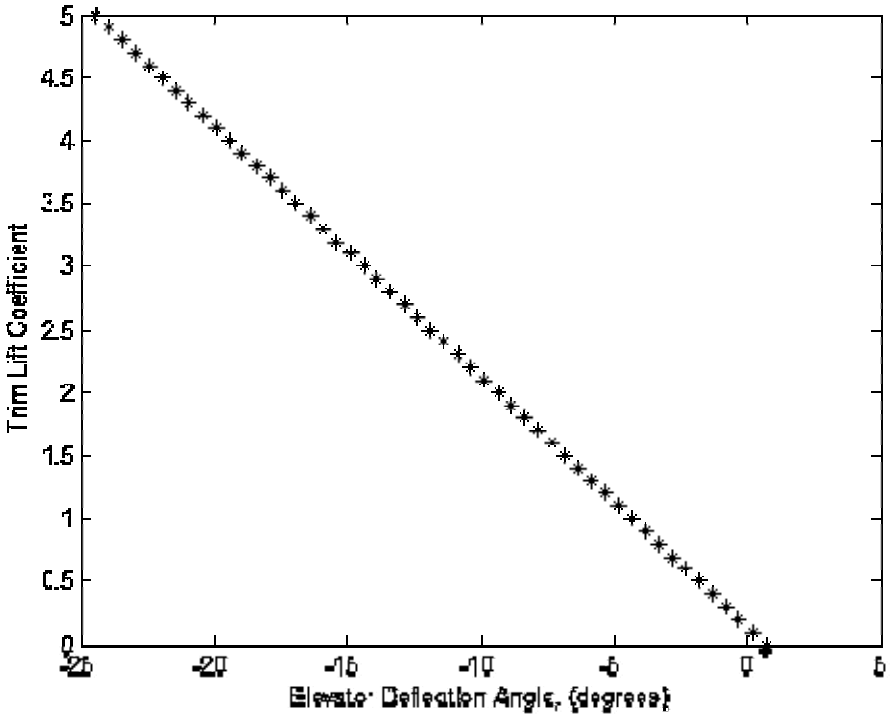

Figure IV.1 Elevator Deflection Required vs. Trim Lift Coefficient During Landing

Stability and control derivatives were found using JKayVLM for three flight phases: cruise, takeoff, and landing as described in Tables IV.3 and IV.4.

Table IV.3 Flight Conditions for Stability and Control Evaluation

Flight Phase	Cruise	Takeoff	Landing
Altitude	30,000 ft	Sea level	Sea level
Speed (Mach)	0.8	0.15	0.14

Table IV.4 Stability Derivatives

Flight Phase	Cruise	Takeoff	Landing
C_{L_α}	8.58355	6.13028	6.12376
C_{m_α}	-1.89640	-0.91434	-0.91265
C_{m}/C_{L}	-0.22093	-0.14915	-0.14903
C_{L_q}	12.33243	10.23329	10.22687
C_{m_q}	-30.99853	-25.62745	-25.60973
$C_{L_{de}}$	3.93983	3.12520	3.12229
$C_{m_{de}}$	-0.56138	-0.30944	-0.30878
$C_{l_{da}}$	-0.65494	-0.54692	-0.54650
$C_{n_{da}}$	-0.00190	-0.00213	-0.00213
$C_{Y_{dr}}$	0.06341	0.07036	0.07037
$C_{l_{dr}}$	0.00475	0.00517	0.00517
$C_{n_{dr}}$	-0.02625	-0.02866	-0.02866
C_{Y_β}	-0.23605	-0.22687	-0.22684
C_{n_β}	0.04377	0.04058	0.04057
C_{l_β}	-0.01726	-0.01348	-0.01347
C_{Y_r}	0.18292	0.17566	0.17563
C_{n_r}	-0.06185	-0.05898	-0.05896
C_{l_r}	0.01013	0.00966	0.00965
C_{l_p}	-0.71055	-0.54909	-0.54859
C_{n_p}	-0.40859	-0.41188	-0.41177

IV.4 Crosswind Landing

The RFP requires a landing in 25 knot crosswind with 5 knot tailwind. This corresponds to a 22 degree sideslip angle, β. The crosswind will cause the aircraft to yaw and roll, so rudder deflection and change in bank angle will be needed. The 5 knot tailwind will reduce the effective velocity of the aircraft causing the need to deflect the ailerons. Using the data from JkayVLM for landing, with a rudder sizing of 30% the chord, the following simultaneous equations (2) were solved, where $C_{Y\delta\alpha}$ was assumed to be 0, and C_W is the weight coefficient.

$$\begin{pmatrix} C_{Y_{\delta a}} & C_{Y_{\delta r}} & C_W \\ C_{l_{\delta a}} & C_{l_{\delta r}} & 0 \\ C_{n_{\delta a}} & C_{n_{\delta r}} & 0 \end{pmatrix} \begin{pmatrix} \delta a \\ \delta r \\ \phi \end{pmatrix} = - \begin{pmatrix} C_{Y_\beta} \\ C_{l_\beta} \\ C_{n_\beta} \end{pmatrix} \beta \qquad (2)$$

The results of this calculation can be seen in Table IV.5.

Table IV.5 Crosswind and Tailwind Required Maneuvering

Situation	Crosswind Landing (25 knot crosswind, 5 knot tailwind)
$\delta\alpha$ (aileron deflection)	-0.1826^o
δr (rudder deflection)	22.9897^o
φ (bank angle)	6.74537^o

Since a maximum rudder deflection of 30 degrees is allowed, there will still be lateral control available from the rudder during landing.

IV.5 Engine Out

Most aircraft are required to be able to land with at least one engine nonfunctional. Having four engines is a large advantage because should one engine go out, another

engine remains opposite the CG. The aircraft can still function even if an outboard engine is lost during flight. A program from the university was used called LDstab. This program estimates stability and control derivatives and engine-out constraints based on required yawing moment coefficient. The most important part of the flight in which analysis of engine-out performance is necessary, is landing. Due to lower speeds, control surfaces are less effective. If the aircraft can still be controlled, even with one engine lost, during landing, all other aspects of flight without an engine can also be done.

LDstab was run using the geometry of the aircraft, the full rudder deflection of 30 degrees, and a bank angle of 5 degrees. From this calculation, a sideslip angle, β, of 1.333 degrees and an aileron deflection, δ_a, of -11.5152 degrees were found.

With these results, the effective aspect ratio of the vertical tail becomes 4.35, and a maximum yawing moment coefficient of 0.1456 is available. This shows that with full deflection, there is still some yawing capability, which is important for controlling the yaw angle during landing.

V. Propulsion & Powered Lift Systems

V.1 Powered Lift Systems

Due to the constraints for landing and takeoff distances, a powered lift system must be used on the aircraft to generate the required lift. Common powered lift systems for other STOL aircraft include vectored thrust, augmenter flaps, Externally Blown Flaps (EBF), Upper Surface Blowing (USB), and internally blown flaps (jet flaps).

Table V.1 shows the maximum attainable values for lift coefficient using the previously mentioned systems.

Table V.1 Powered Lift Comparison

System	C_{Lmax}
Vectored Thrust	3
Augmenter Flap	7
Externally Blown Flap	7
Upper Surface Blowing	8
Internally Blown Flap	9

The C_{Lmax} required for landing, 3.8, was compared to the values seen in Table V.1. To determine which powered system was to be used, a brief analysis was conducted to determine the best fit for the mission requirements.

Vectored thrust utilizes a 1-D or 2-D variable nozzle to redirect thrust in the desired direction. However, due to deflection limitations with the variable nozzle, angling the nozzle at its maximum downward deflection has only been proven to raise C_{Lmax} to 3. A vectored thrust system can be seen in Figure V.1.

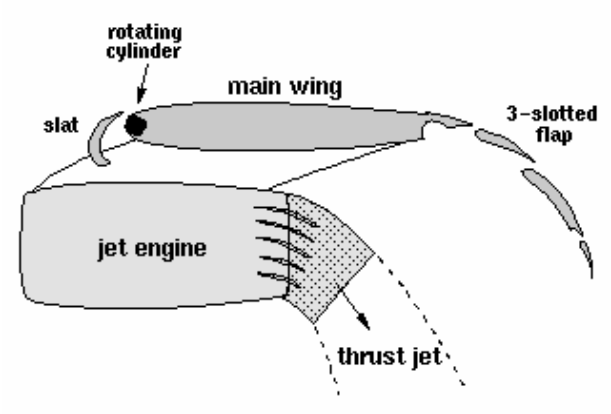

http://www.aerodyn.org/HighLift/powered.html

Figure V.1 Triple-Slotted Flap System

Augmentor and EBFs, as seen in Figure V.2, require large multiple slotted flaps to extend downward into the exhaust of the engines. As flow travels over the flaps, it is accelerated, resulting in an increase in lift. Externally blown flaps are a proven technology that is currently in use on the C-17.

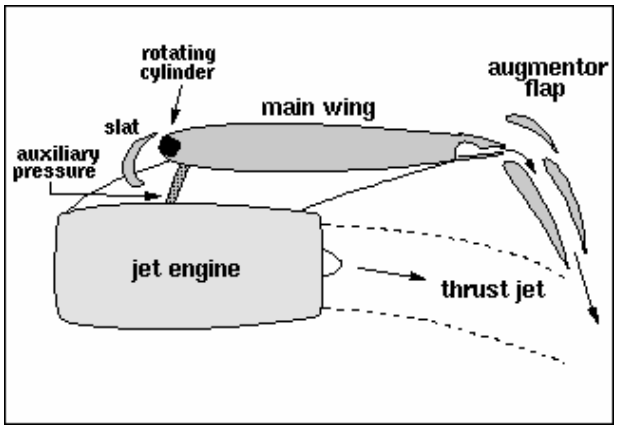

http://www.aerodyn.org/HighLift/powered.html

Figure V.2 Augmentor Flap System

USB requires mounting the engines on top of the wings, to take advantage of the Coanda affect to get extra lift. While USB has shown great potential in testing, there are still no US production aircraft that utilize this technology. In order to optimize the flow over the wing at different flight conditions, variable geometry nozzles are required, or large

inefficiencies will result. There are also known issues with USB at high speeds due to the altering of isobars over the wing. A USB system is shown in figure V.3.

Figure V.4 An-72 with USB
http://www.aeronautics.ru/archive/vvs/an72-01.htm

Internally Blown flaps, or jet flaps, as shown in figure V.43, have shown remarkable promise in not only high lift systems but also in controlling the aircraft. However, by their very nature of routing jet exhaust through the flap, they are not only costly to develop and build, but also difficult to maintain.

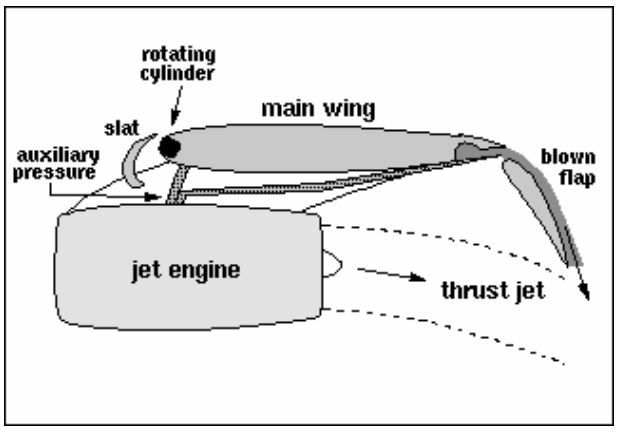

Figure V.4 Internally Blown Flap System
http://www.aerodyn.org/HighLift/powered.html

Externally Blown Flaps were chosen for each concept, as well as the final design, due to their proven track record, ability to reach the required lift coefficients, and allowing for a

conventional design. Maintaining simplicity at each step, not only the lowers cost, but the ease of maintenance can also be passed onto the customer.

V.2 Propulsion

Engine selection plays a key role in ensuring that the *Free-Weight* will meet all required criteria. In the case of this STOL cargo aircraft, an engine configuration is needed that can cruise at Mach 0.8, climb and maneuver with a 240,000 lb airframe, and more importantly, be able to create enough rolling speed for a takeoff with 2500 ft. To meet these objectives it was first necessary to analyze what other modern day cargo aircraft used for propulsion and their corresponding capabilities. With the thrust to weight ratios, fuel consumption, range, and max speed data from other aircraft, the initial concepts can be analyzed.

The most modern large cargo aircraft in the United States Airforce today is the C-17 Globemaster. An aircraft with the ability to take off in 3000 ft, cruise at Mach 0.7, and carry heavy loads, it is a good starting point for comparison. An aspect that immediately jumps out about the C-17 is its engine configuration of 4 high bypass ratio turbofans, a decision that weighed heavily on this design. Having a two engine configuration would result in a lighter and cheaper aircraft, with less required maintenance. Yet the aircraft to be designed must operate under combat conditions, and take off within 2500 feet. Having an engine out could be disastrous in a two engine configuration. The minimal thrust required for takeoff and cruise will be analyzed in a later section.

Other aircraft used for comparison were the C-141 Starlifter, An-70, and the Il-76D, each a high capacity, cargo aircraft. All of these aircraft were analyzed in the comparator aircraft section previously.

As seen in the table above, the most common thrust to weight ratio is near .3, with max thrust to 141,000 lb. With common configurations of similar aircraft compared, it was then possible to analyze the two initial design concepts.

V.3 Engine analysis

For any aircraft, the choice of engines comes down to satisfying the required constraints with minimum cost and weight penalty. The engine choices for this cargo aircraft can be effectively limited to turbofan engines, with some degree of bypass, as the aircraft will not enter the supersonic flight region. Also, as the required cruise speed is set at Mach .8 at altitude, this eliminates all prop engines, even propfans, which in recent years have shown remarkable performance with astonishing fuel savings. Unfortunately, the most powerful propfans to date, the Ukrainian D-27s that powers the An-70, are only capable of propelling an aircraft to Mach 0.76, just short of mission requirements. A comparison of the medium and low bypass ratio engines can be seen in Table V.2.

Table V.2 Engine Bypass Ratio Comparison

BPR	Inlet Mass flow	Weight (lb)	Length (in)	Diameter (in)
2	850	5388	100.7	65.6
6	1350	7993	129.0	82.7

Two engines, one low bypass and one medium bypass turbofan, were analyzed for weight, size, and performance at all mission segments. The performance of each was

broken down into maximum thrust provided at takeoff, with corresponding fuel consumption, and fuel consumption at cruise speed. With these values, a choice was made to pick the medium bypass ratio engine, with a BPR of 6, over the low bypass engine of BPR 2. After the engine was decided upon, it was then be possible to scale it to ±20% of the engines size and performance to fully meet the mission requirements. Table V.3 shows a comparison of the low and medium bypass ratio engines for different aspects of the mission.

Table V.3 Mission Segment Analysis Based on a 4 Engine Configuration

	Takeoff			**Cruise M=.8**		
BPR	Max Thrust (lb)	SFC (lbf/lb/hr)	Fuel Flow (lb/hr)	Thrust (lb)	SFC (lbf/lb/hr)	Fuel Flow (lb/hr)
2	41965	.532	22306	4069	.820	3337
6	42046	.354	14896	4000	.715	2860

At sea level for takeoff and landing, the BPR 6 engine has a huge advantage over the BPR 2 engine in TSFC, as seen in the chart above. However, the bypass ratio of 6 did not garner as impressive of fuel savings at the cruise velocity as expected. This is largely due to the drag increase at Mach 0.8 due to the larger cross section of the engine, resulting in less net thrust. To overcome the weight difference of the larger engine size and the additional required structure, over 13,000 lb for 4 engines, 13,000 lb of fuel would have to be saved in the FDAV mission. Table V.4 shows a comparison is fuel consumption fot the two bypass ratio options.

Table V.4 Fuel Consumption Comparison

BPR	**Engine Fuel Consumption**
2	63000 lb
6	54000 lb
Difference	9000 lb

After analyzing the fuel consumption rates based on the two main FDAV mission segments, there was only a fuel savings of 9,000 lb, 4,000 lb short of justifying the larger engines. The fuel consumption was calculated using a mission program and shows the total fuel required to takeoff, land, drop of cargo, and return home with 5% trapped fuel and reserve fuel remaining. The BPR of 2 engines will be used, despite the higher fuel costs, as weight savings are essential for takeoff and particularly on landing, where fuel will be near empty with both engine types, but with one airframe weight almost 13,000 lb greater than the other.

The engines themselves were scaled down 20% to save size and weight, while still generating the thrust required for takeoff and cruise. The fuel consumption numbers in the section above are indicative of that scaling. Final engine size is shown below with cowling. Notice the cowling is of a symmetrical design, as it does not require added room for the accessory gearbox due to the use of an electronic control system, which will be described with electrical systems below. This symmetric cross section helps to reduce nacelle drag by as much as 6%, with a slight reduction in weight as well.

A main point of optimization is the cruise altitude for the aircraft. This is based on the optimal altitudes for not only the engines fuel efficiency, but also the aircraft's drag. To

provide a starting location for the mission program TSFC was plotted vs thrust at potential cruising altitudes, shown in Figure V.5 below.

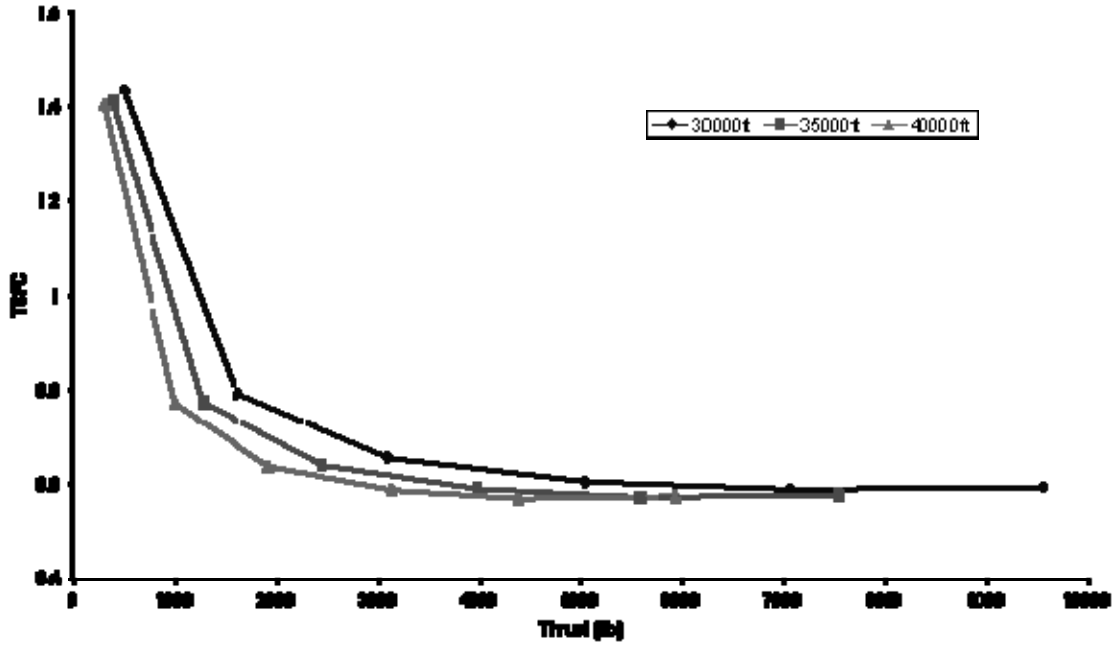

Figure V.5 Engine Performance Parameters at Potential Cruise Altitudes for BPR2

The 30,000 ft required minimum altitude is clearly not optimal, as TSFC can be substantially lowered by flying between 35,000 ft, and 40,000 ft. With these altitudes in mind, further optimization will be concluded in the flight performance section of the report.

V.4 Starting and Electrical Systems

To save weight and maximize engine performance, bleed air will not be taken out of the main engines, a proven design method on the Boeing 777. Where pneumatic devices were once used, electric systems will take their places. For the *Free-Weight*, pneumatic actuators will be replaced with electric hydraulic actuators, de-icing systems will be electro-thermal in nature instead of utilizing hot engine bleed air, and cabin climate

control systems will use electricity instead of having to first cool and decelerate engine air for use in cabin. The aircraft will be started using the electric generators mounted on the engines themselves, and using them as starters by pumping DC current into them from the APU. This will require that the generators themselves put out power in variable frequencies, requiring an additional power converter to condition power for usage by the electrical components of the aircraft. This converter will be placed above the forward bulkhead of the cargo bay. Figure V.6 shows a schematic of electrical usage on the *Free-Weight.*

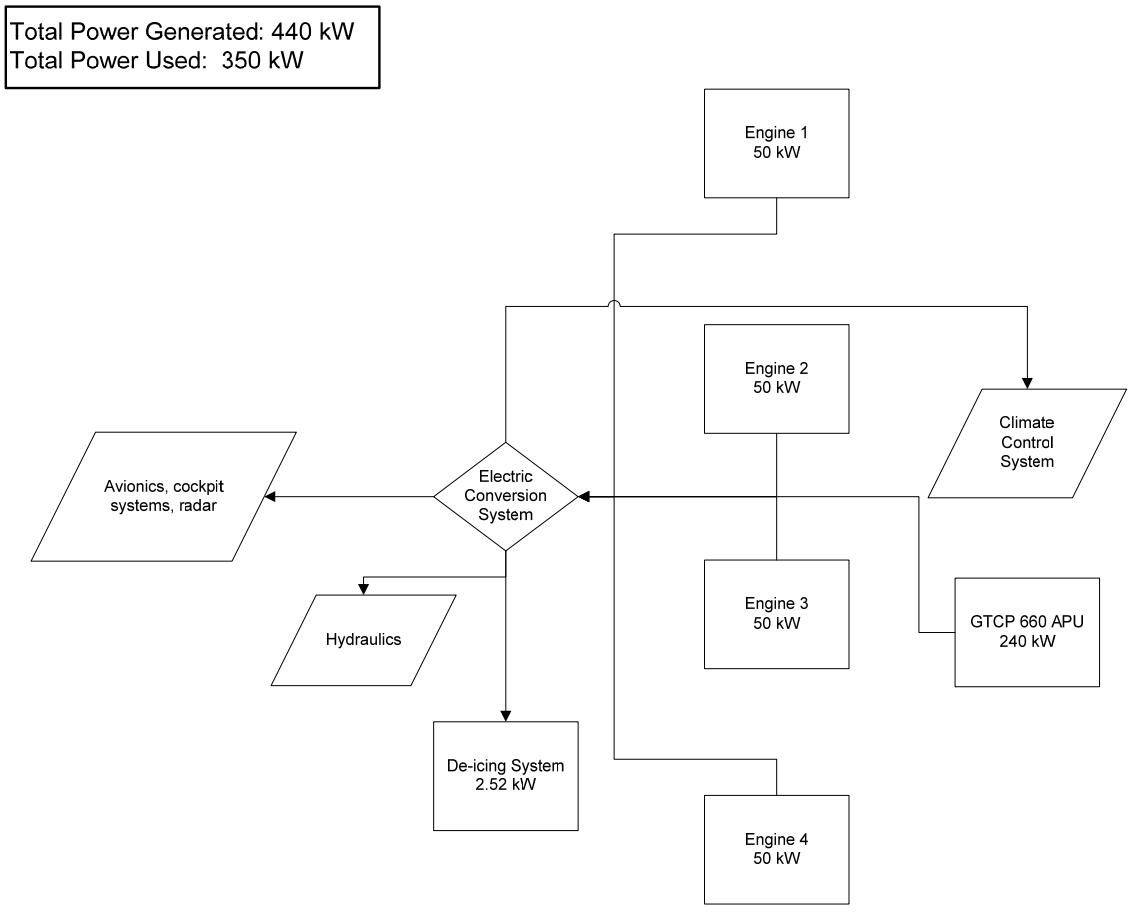

Figure V.6 Electrical Usage Schematic

V.5 Auxiliary Power Unit

An APU is required for the FDAV mission, as the aircraft will be landing on an unfinished airstrip and will not have access to a ground cart. After the initial aircraft configuration was completed, it was decided that the APU was to be placed in the rear of the landing gear pod, thus limiting the possible size of the APU to be selected. Based on the amount of power required and size constraints of the gear pods, a GTCP 660 series APU derivative was selected. The APU will be a 20% scaled down variant of that used on the 747, capable of putting out 240 kW while weighing only 440 lb and having a maximum diameter of less than 4 ft. Table V.5 shows the specifications of this device.

Table V.5 APU Specifications

Auxiliary Power Unit						
Specs	**Length (in)**	**Width (in)**	**Height (in)**	**Power (kW)**	**Weight (lb)**	**Fuel Flow (lb/hr)**
GTCP 660	60	32.4	43.6	240	432	500

The APU will start the engines with its outputted electrical power, and will supplement the engines output of electricity under heavy loads.

VI. Airframe Structures

The structure of the *Free-Weight* must be designed to withstand the extreme loads imposed upon the craft by the RFP short take-off and landing requirements. The aircraft will experience very high stress during routine operations due to the high lift required for take-off and landing on a short field with a substantial payload. The *Free-Weight*'s structure must be handle the high loads associated with the STOL requirements while having a minimum of structural weight. The airframe will utilize advanced materials to increase structural strength and minimize weight as compared to traditional aircraft materials. The austere field conditions also dictate that structure should be rugged enough to avoid excessive injury during a rough landing, and easily repairable in the event such damage does occur.

VI.1 Materials

The materials for the structure of the *Free-Weight* transport must be chosen to decrease the total weight of the aircraft without sacrificing the material properties. The materials used must be strong enough to withstand the various stress and loading scenarios that exist in certain areas of the aircraft structure. The plane will experience high loads due to the high lift systems as well as the increased g-forces at take off and landing as required for a STOL capable aircraft.

The materials chosen for the *Free-Weight* have to be able to withstand environmental effects such as corrosion and lightning strikes. The areas of the wing and flaps affected by engine exhaust must also be able to withstand elevated temperatures. In addition, the

external structure of the aircraft must be impact resistant to land in austere fields without becoming damaged. The structure should also be easy to inspect and repair in the event of a bird strike or damage from objects in the field.

To this end, the materials chosen for this aircraft combine the traditional, tried and true materials of aircraft design, such as aluminum and titanium alloys, with more innovative material technology, such as composites and advanced alloys. This combination will decrease the overall weight of the aircraft as well as improve inspection, maintenance, and repair.

Aluminum alloys are the predominant material in use in the aircraft industry today. While new technology will play an important part of this aircraft, aluminum alloys will still make up a sizable part of the structure. Aluminum offers a good strength to weight ratio. It is susceptible to stress corrosion, however. The standard use of these materials makes repairs and inspection easier for mechanics who are already experienced with their use.

Aluminum lithium, an aluminum derivative known as Al 2090, offers a roughly 8% weight savings and 10% increase in strength over standard aluminum alloys. This material also has the advantages of being very impact resistant as well as highly weldable, further decreasing weight by decreasing the number of fasteners required for use. This alloy also has a high resistance to corrosion and has a lower crack growth rate than standard alloys, making it an excellent choice for the exterior of the aircraft. There is some increased manufacturing cost associated with the relatively high likelihood of

defects in the final product due to the thermal conductivity of Al-Li and the possibility of localized strain, however manufacturing processes are continuously improving, driving cost down [Ref 8].

Another fairly standard material used in aircraft structure is titanium alloy. Despite a higher density, titanium alloys offer a roughly 10% weight decrease over aluminum parts due to their increased strength. Titanium alloys are also very good for higher temperature applications.

The *Free-Weight* will also incorporate glass reinforced fiber metal laminate, or GLARE, which combines thin sheets of aluminum bonded to sheets of S-glass fibers embedded in adhesive. Being a composite, GLARE offers the ability to tailor its properties. A roughly 10-20% weight savings over aluminum is gained in addition to offering excellent cyclic fatigue properties and impact resistance. Repairs can be made using riveted patches, similar to standard aluminum alloys, or by using a bonded patch. Both methods are widely used by the Air Force, not requiring mechanics to learn new techniques. [Ref 34] Damage is also easy to detect, usually failing in the same manner as aluminum, rather than interlaminarily. Although the manufacturing costs associated with this relatively new material can be cost-prohibitive, increased use and experience with this material will most likely decrease the cost in the upcoming years, especially as this material is seeing application in the Airbus super-jumbo, the A-380.

Another composite material that will be used on this aircraft are carbon fiber reinforced polymers, or CFRP. Property tailoring, combined with excellent strength to weight properties and increased fatigue capabilities can provide about a 20% weight decrease over aluminum. These materials can also be attached through a bonding process rather than using fasteners, reducing weight. Manufacturing and tooling costs, as well as initial development costs, can be high for CFRP materials. Increased experience with this material in the aerospace industry on such planes as the 787 and the fact that there is little manufacturing waste associated with composites are lowering the cost of this lightweight, high strength material.

CFRP composites are thermoset, meaning they cannot be reworked once cured. However, thermoplastic matrix composites, TPMC, can be reworked indefinitely due to their lower manufacturing temperatures. Thermoplastics are far more impact resistant and less likely to experience interlaminar delaminations than standard thermoset composites. The easy workability of thermoplastics also decreases the manufacturing costs and allows damaged parts to be reformed and used again. Although still relatively new, these materials are seeing use in many Airbus aircraft due to their impact resistibility and weight savings of roughly 20% compared to aluminum. Unlike other newer materials, the cost is only moderately above that of aluminum due to the manufacturing and processing ease.

Overall cost and property information for the aforementioned materials can be seen in Table VI.1.

Table VI.1 Material Characteristics [Ref 22, 4, 35]

Material	Ultimate Strength (ksi)	Yield Strength (ksi)	Toughness (ksi√in)	Density (lb_m/in^3)	Modulus, E (10^6 psi)	Shear Modulus, G (10^6 psi)	Cost ($)
Al 2024-T3	70	50	40	0.1	10.6	4.06	2.5
Al 7075-T6	83	73	26.4	0.102	10.4	39	3
Ti-5Al-2.5Sn	125	120	87.4	0.162	16-18.1	6.96	23
Ti-6Al-4V	170	160	39.1	0.160	16.5	6.38	21
Al 2090-T83	79.8	75.4	40	0.0936	11	4.06	12
GLARE 2 (3/2)	176	52	-	0.091	9.6	2.21	
CFRP	110/4	-	21-41	0.061	32/1.0	-	100
FORTRON PPS TPMC	29	24.9	-	.0578	1.8	-	-

The previously discussed materials will be used as shown in Figures VI.1 and VI.2 and explained in further detail in the following sections.

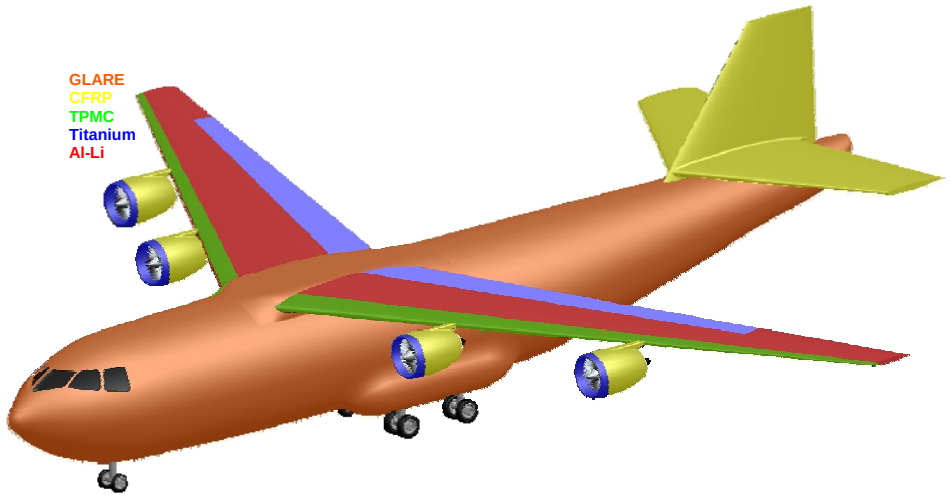

Figure VI.1 External Material Usage on *Free-Weight*

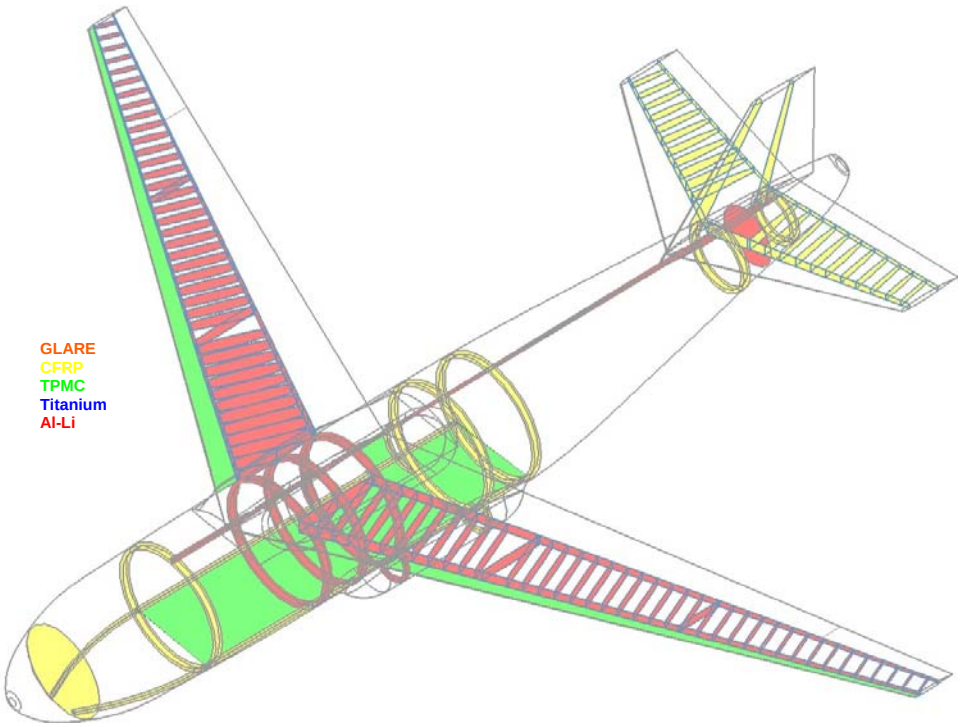

Figure VI.2 Material Usage on *Free-Weight*

VI.2 Loading

The structure of the *Free-Weight* must be able to withstand the maximum loads experienced by the plane, not only during normal flight, but also the loads encountered during extreme cases such as gusts, maneuvering and landing. MIL-A-8861B, reference 23, specifies that the aircraft must be able to function up to a limit load factor, N_z, of 2.5 and -1 and an ultimate load factor of 3.75 and -1.5 for the a fully loaded plane. The same military specification, states that the aircraft must endure gust velocities of 66 ft/s at turbulent gust penetration speed, 50 ft/s at max level flight speed, and 25 ft/s at the limit speed. The *V-n* diagram of the *Free-Weight*, when fully loaded, is shown in figure VI.3. Both the full flaps, C_{Lmax} of 3.8, and no flaps, C_{Lmax} of 1.72, cases are shown.

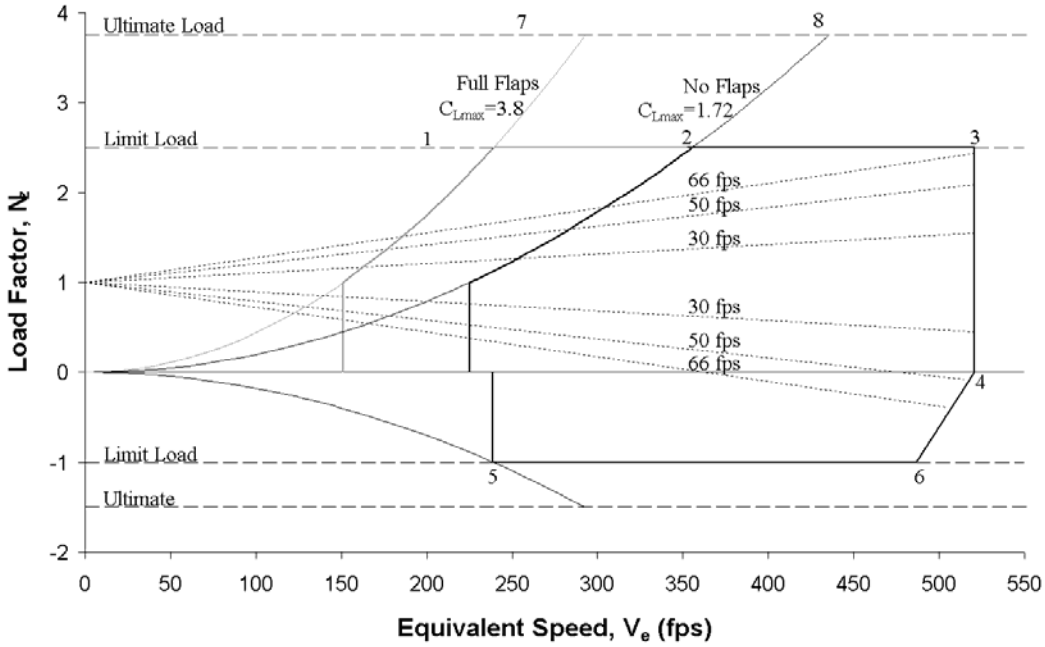

Figure VI.3 *V-n* Diagram

As can be seen in the diagram, the gust loads are not the restricting factors of the design, having a lower maximum load factor than the limit load factor. The corner points of the diagram show the extremes to which the structure must be designed for. Corner points are listed in table VI.2.

Table VI.2 V-n Diagram Corner Points

Point	V_e (ft/s)	N_z
1	239	2.50
2	352	2.50
3	521	2.50
4	521	0.00
5	239	-1.00
6	487	-1.00
7	435	3.75
8	257	3.75

For the normal load factor, N_z of 1, and assuming an elliptical lift distribution over the wing, the aerodynamic loading of the *Free-Weight* appears in Figure VI.4.

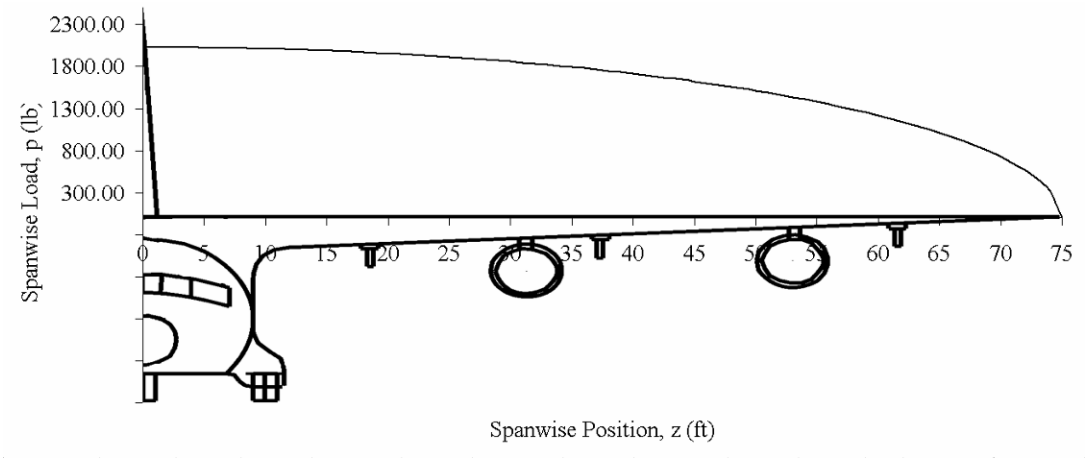

Figure VI.4 Elliptical Wing Loading

VI.3 Wing Structure

The wing structure for the *Free-Weight* is a 2 spar design. The forward spar is located at 15% of the chord, while the rear spar is located at 65% of the chord. This allows room for the leading and trailing edge flaps which require at least 10% and 30% of the chord, respectively. The additional 5% of the chord at either end of the wing box will be used for flap control mechanisms. This spar placement is within the normal range for transport aircraft as seen in Roskam's reference 26 and also allows plenty of room for fuel placement within the wings.

The wing loading for each of the spars, as well as the total loading, can be seen in Figure VI.5. This was found by summing forces and moments around the center of pressure to find the lift acting on each spar. The center of lift changes for each angle of attack, so at zero angle of attack, the rear spar is more engaged, while at increased flight angles, the front spar becomes more engaged. This chart represents the ultimate loading factor of 3.75 while the aircraft is at a 5 degree angle of attack.

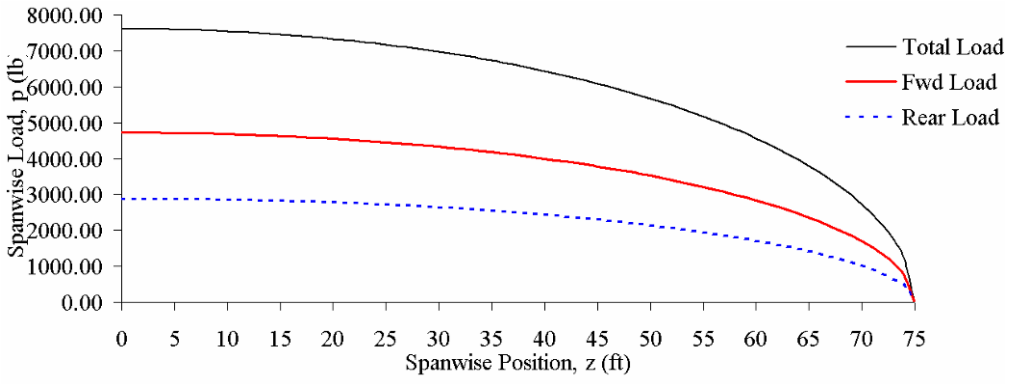

Figure VI.5 Wing Loading for the Forward and Rear Spars

From this loading scheme, the shear force and bending moments on each spar were calculated which can be seen in Figures VI.6 and VI.7. Engine weight was factored into the calculations, by including a 9510 lb downward force at each engine location.

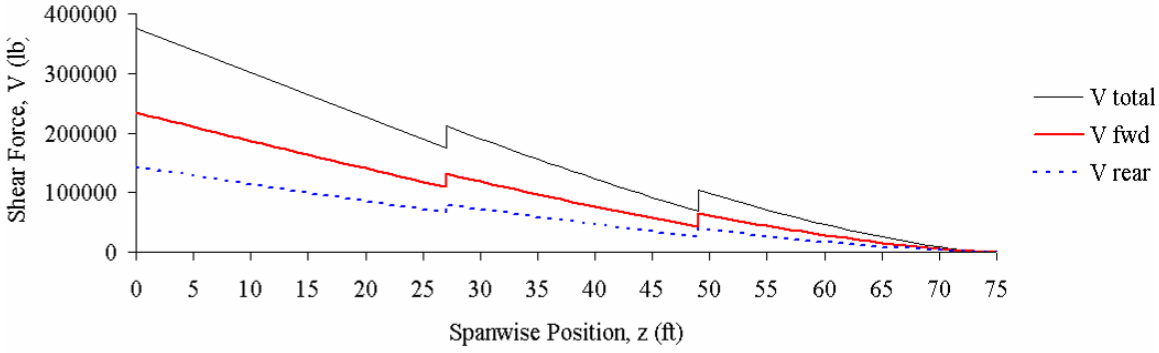

Figure VI.6 Shear Force Diagram for the Forward and Rear Spars

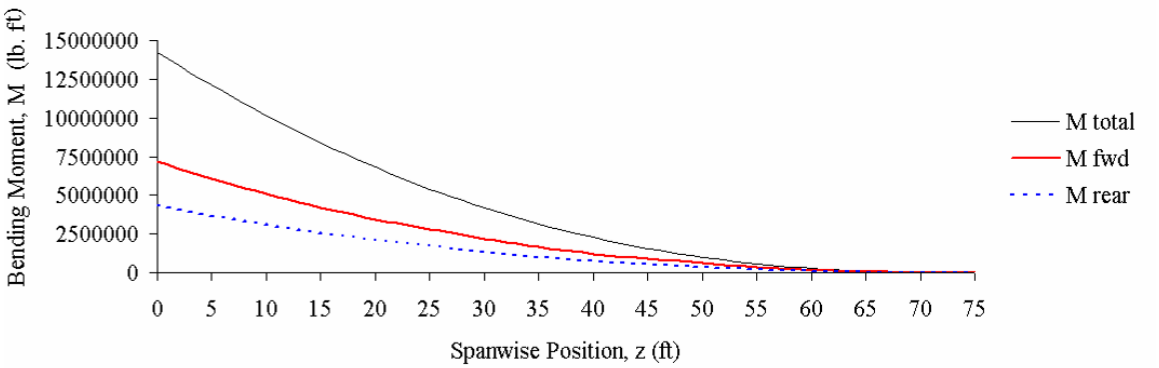

Figure VI.7 Bending Moment Diagram for the Forward and Rear Spars

The spar thickness was then determined using equation (VI.1), resulting in Figure VI.8. This figure shows the minimum cross-sectional area of each spar required for the load conditions for an aluminum spar.

$$A_c = \frac{M}{\sigma_u h} \quad \text{(VI.1)}$$

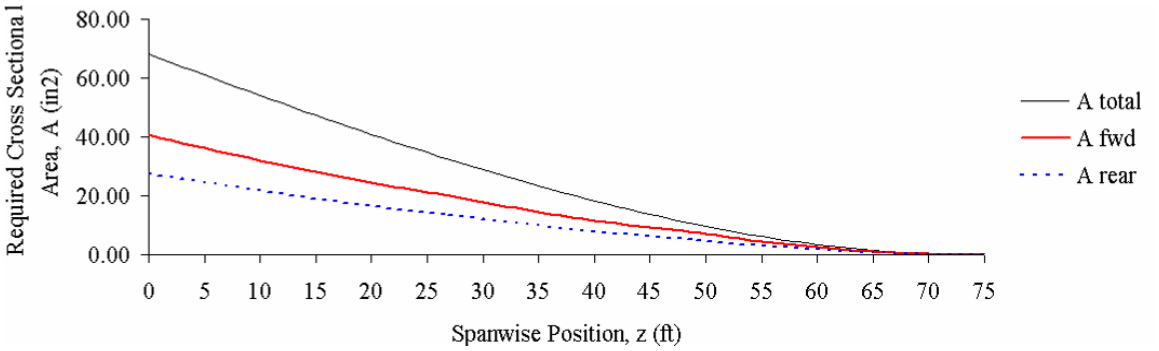

Figure VI.8 Minimum Cross Sectional Areas Required for Forward and Rear Spars

Comparing several angles of attack, the required maximum thickness for a rectangular, tapered spar is about 4 inches for both the forward and rear spars. This thickness decreases with the use of advanced materials and more efficient spar shapes, such as an I-beam.

The ribs are placed perpendicular to the rear spar at 24 inch intervals, except for the two main ribs at each engine location. These ribs, located 26 ft and 48 ft along the wing span, are parallel to the flight direction and have a heavier structure to support the engine loads. Rib and spar placements are common for large transport aircraft and were determined using the methods discussed by Roskam in reference 26. Ribs and spars of the aircraft wing will be constructed of aluminum lithium alloy to reduce weight while still withstanding the lift loads. The wing structure can be seen in Figures VI.9 and VI.10.

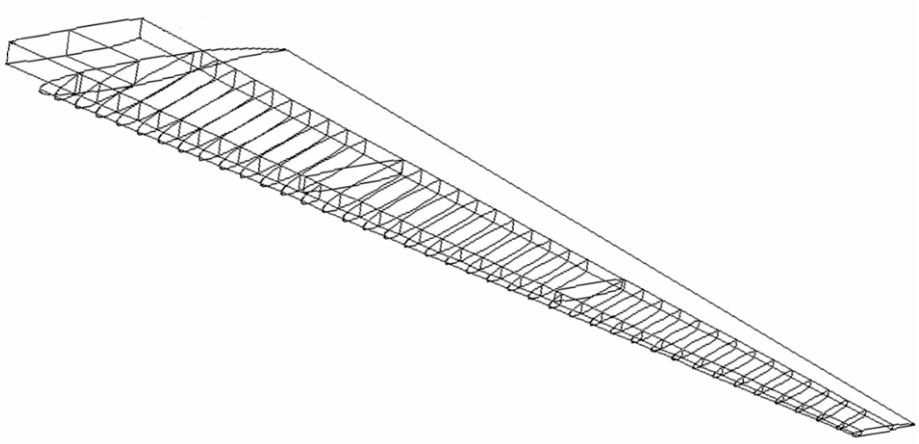

Figure VI.9 3-D Wing Structure

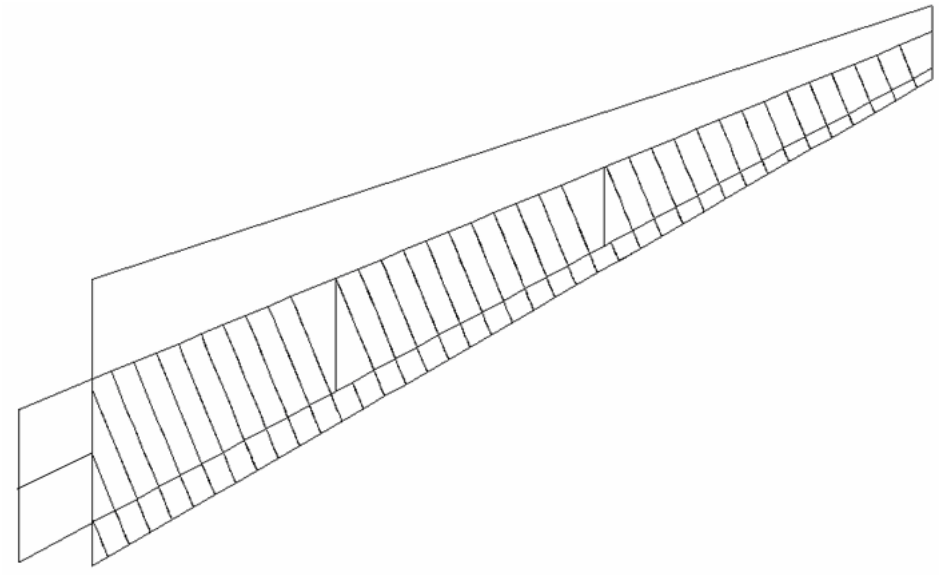

Figure VI.10 2-D Wing Structure

The wing skin is integrally stiffened with blade section stiffeners. This is a fairly common arrangement, already widely used, helping to decrease weight by reducing the number of fasteners [Ref 23] The wing skin will be constructed of Aluminum-Lithium Alloy, Al 2090-T83.

The wing box is a carry-through design. The portion of the wing box within the fuselage will feature an additional spar to help relieve the stress on the structure where the wings

connect to the fuselage. The leading edge of the wing will be made of TPMC composites to help resist impact damage and save weight.

VI.4 Fuselage Structure

The fuselage has a total of 10 major bulkheads, spaced so as minimize the number of bulkheads required for highly loaded areas of the structure. Where possible, bulkheads are shared by structure with is affected by high loads, such as the wing spars and landing gear. Bulkheads will be made of either CRFP composites or aluminum lithium alloy. The forward- and rear-most bulkheads are pressure bulkheads. These will be domed rather than flat, to decrease the amount of structure required to withstand cabin pressurization. The function and position of each major bulkhead is listed in Table VI.3.

Table VI.3 Bulkhead Locations and Functions

Bulkhead Number	Function	Station (in)
1	Forward pressure bulkhead	96
2	Cabin Door / Fwd Cargo Bay / Landing Gear Support	300
3	Forward Wing Spar	498
4	Center Wing Spar	574
5	Rear Spar	642
6	Rear Landing Gear Support	810
7	Cargo Door Actuator / Rear Door Support	900
8	VT and HT Forward Spars	1337
9	Rear Pressure Bulkhead / HT Tail Actuator Support	1389
10	VT and HT Rear Spars	1442

Two longitudinal beams run beneath the aircraft floor from bulkhead 1 to bulkhead 7, providing support to the cockpit and cargo floors. These beams will be constructed of CFRP composite. In the cargo bay, a grid work of floor beams connected to the

longitudinal beams supports the cargo floor and FDAV or other cargo. A larger Keelson beam runs through the upper fuselage, from bulkhead 2 to bulkhead 10, providing a majority of the fuselage bending strength. The cargo floor is made up of a sandwiched thermoplastic composite to better resist damage from frequent loading and unloading of the payload required by the RFP. The fuselage was designed using Niu's design methods in Reference 23.

The cabin will be pressurized to an altitude of 7000 ft, which corresponds to an atmospheric pressure of 11.34 psia. The plane will also have a maximum altitude of 40000 ft which corresponds to 2.73 psia. This results in a maximum pressure differential of 8.61 psi. The stresses for different layups of GLARE material were compared using equation VI.2.

$$\sigma = \frac{pr}{t} \quad \text{(VI.2)}$$

The required material properties were more than met by the capabilities of GLARE 2 (3/2). The GLARE skin panels will be 0.049 inches thick over the majority of the aircraft, with pad-ups at higher stress areas such as door surrounds. The skin and stringers resist the pressure differential between the aircraft and the atmosphere at altitude. The unidirectional GLARE 2 composite can also be positioned at an angle to resist not only the internal pressure but also some of the fuselage bending. This would decrease the required size of the Keelson beam.

VI.5 Tail Structure

The vertical and horizontal tails are both 2 spar designs with the forward and rear spars positioned at 15% and 65% of the chord, respectively. Ribs are spaced 24 inches apart. The horizontal and vertical tails share bulkhead connections, to decrease the number of bulkheads required for the tail section. The horizontal tail is fully adjustable, which requires additional bulkhead support for the actuator. The actuator support bulkhead is also the rear pressure bulkhead. The tail will be constructed primarily of CFRP composites to decrease weight.

VII. Aircraft Systems and Avionics

The goal in developing the systems and avionics for the aircraft was to provide the necessary equipment to successfully complete the mission objectives while keeping pace with technological advances. Constraints to the systems utilized included using pre-developed equipment whenever possible to minimize cost, and complying to military specifications. The following is an overview of the systems chosen and the functions these individual systems perform, as well as a layout of the cockpit avionics.

VII.1 Counter Measure Systems

Several pre-existing counter measure systems were selected to provide both electronic and physical protection from various missile based threats. These systems' primary purposes are to warn the crew and help defeat both infrared and radar based missile systems.

The countermeasure dispensing unit assembly consists of 3 AN/ALE-47 Countermeasure Dispensor Systems, CMDS, set up with one facing downwards from the underside of the aircraft's fuselage and one on either side of the aircraft's fuselage. This setup provides a highly effective cover pattern by dispensing countermeasures both behind the fuselage and behind the wing mounted engines to best mask the heat signature of the aircraft [Ref 20]. These dispensing units were chosen based on their current use in other comparable USAF aircraft and for their ability to dispense both infrared defeating flares and radar defeating chafes in both manual and automated modes.

Other countermeasure systems chosen for the aircraft include an AN/AAR-44 missile warning receiver. This device detects and tracks multiple IR based threats and alerts the crew. The AN/AAR-44 can also automatically release countermeasures from the dispensor [Ref 17]. An AN/ALQ-156 radar missile defense system provides similar functions, but instead protects against radar based missile systems (BAE). An AN/ALQ-204 Matador IR countermeasure system automatically attempts to defeat IR based missile threats [Ref 17]. Finally an AN/ALQ-196 jammer is an internal, automated countermeasures set which attempts to counter Low Band SAM and AAA threats [Ref 20].

VII.2 Navigation Equipment

The AN/APN-241 Airborne Radar system was selected as the radar system for the aircraft. This dual-channel mono-pulse unit provides the following modes: Weather(WX), WindShear, Ground Mapping, Skin Paint, Beacon Mode (BCN), Station Keeping (SKE), Flight Plan (FP), Traffic Collision Avoidance System (TCAS).

An AN/APN-232 Combined Altitude Radar Altimeter was chosen as the primary altimeter as it is the standard unit for the USAF [Ref 17]. An LN-251 INS/GPS System provides GPS information for navigation purposes [Ref 17]. An AN/AAQ-17 Infra-red detecting set serves a military grade Forward Looking Infrared (FLIR) system complements the night vision of the pilots enabling the crew to see clearly in otherwise inoperable conditions.

VII.3 Communications

Two AN/ARC-210(V) Multimode Integrated Communications Systems were chosen to provide both the pilot and the copilot with the necessary communication tools.

A schematic, seen in figure VII.1, shows the layout of the aircraft cockpit and the locations of the equipment detailed previously.

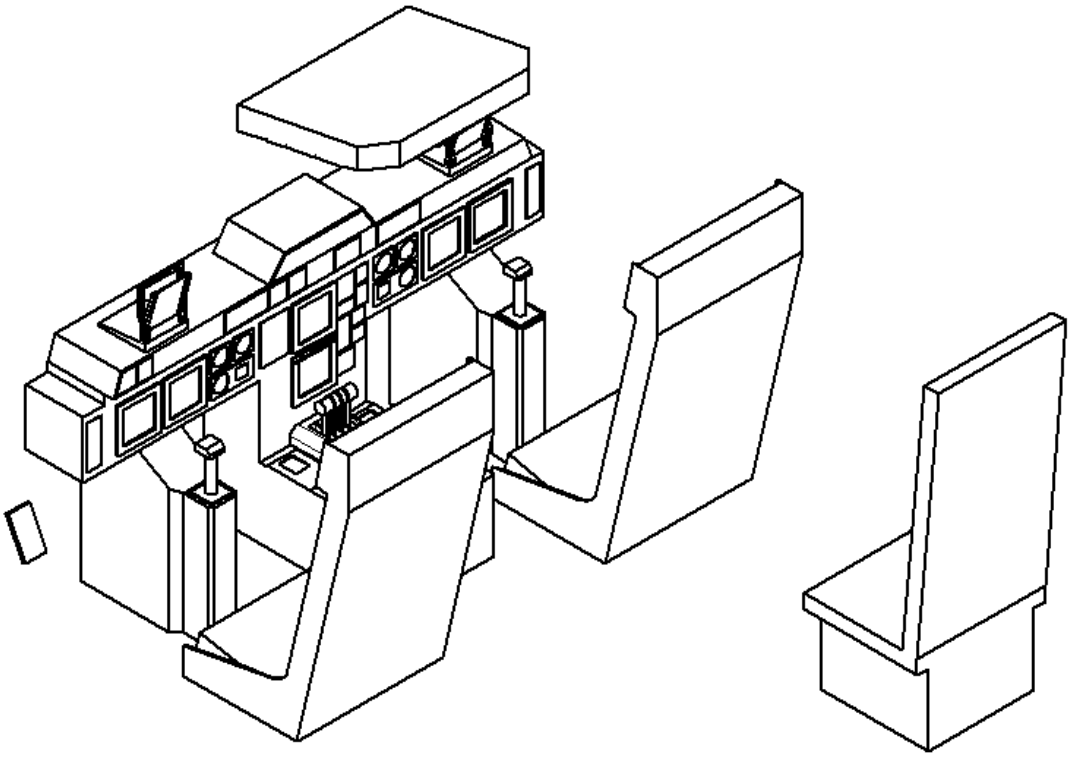

Figure VII.1 Interior Cockpit Layout (A)

Figure VII.2 shows a full cockpit layout, including crew station and lavatory positions.

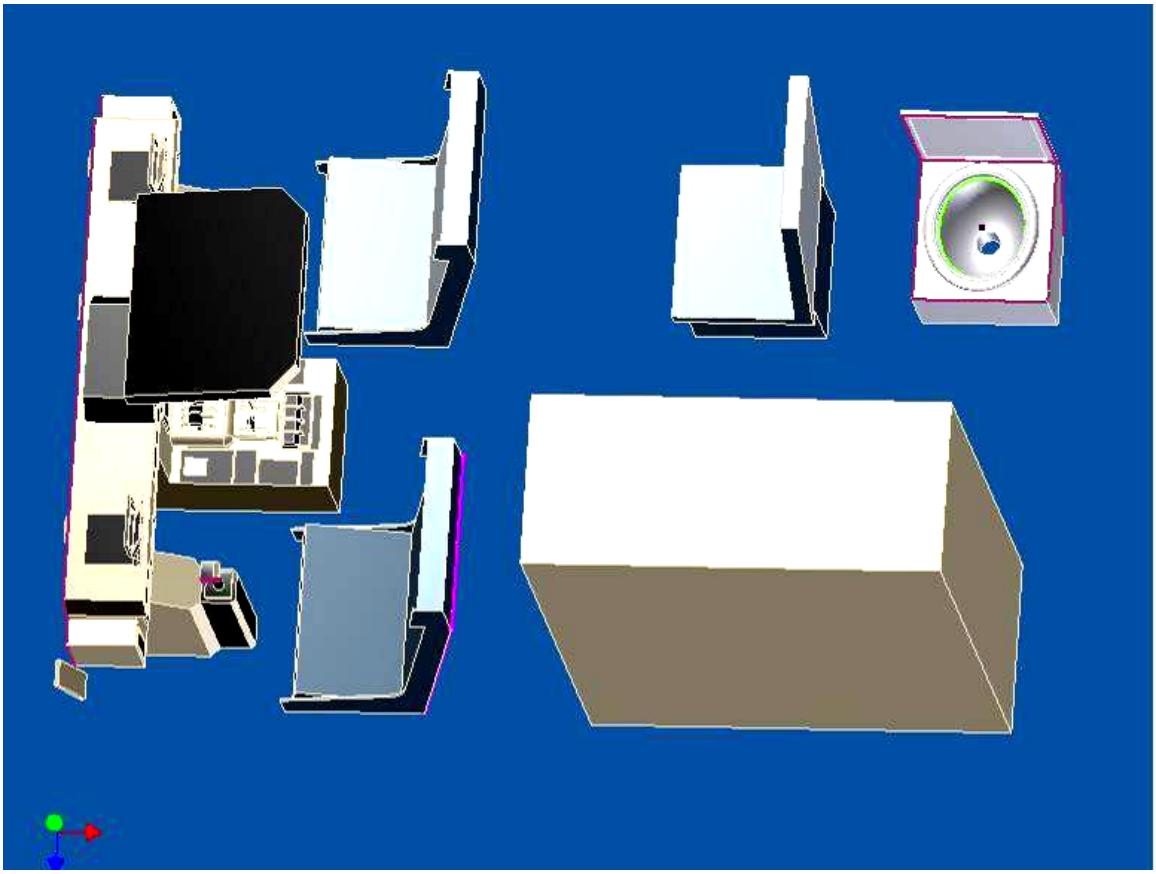

Figure VII.2 Interior Cockpit Layout (B)

A detailed view of the instrument locations on the control panel can be seen in figure VII.3.

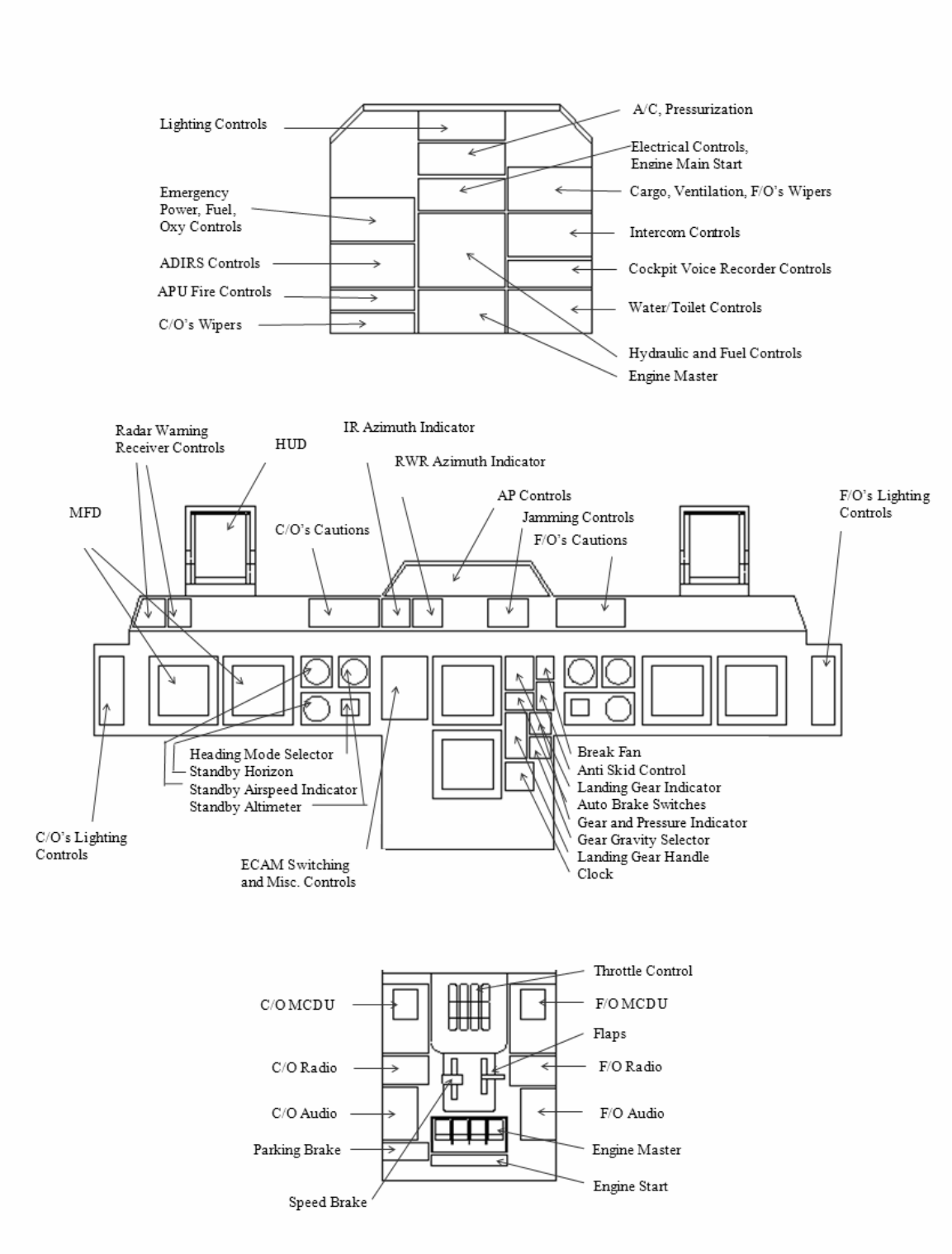

Figure VII.3 Control Panel Layout

VII.4 Fire, Air, Icing Systems

The aircraft's fire protection is composed to two components. The Ansul Cleanguard handheld extinguisher will provide electrically non-conductive and bio-friendly protection for the cockpit. The rest of the aircraft will be automatically monitored by the Ansul INERGEN system which utilizes inert agents, and a quick detection and reaction system that are both electrically safe and people friendly as well.

The air conditioning and pressurization system will consist of the typical systems in place on cargo and commercial aircraft. Bleed air will be directed from different stages of the four engines into two heat exchangers. From there it will be led through an air cycle Machine underneath the flight deck which will perform a refrigeration cycle on the air and send it through a mix manifold. From there the air will be circulated by fans through the flight deck and the cargo area. The flight deck and cargo area will both be pressurized to 8,000 ft atmospheric conditions. In addition, the flight deck will contain a 25 L oxygen converter for pilot and co-pilot, and a separate 25 L converter will be placed in the cargo area for the load master.

The aircraft will feature an electric de-icing system from Cox & Company Inc. This system, called an Electro-Mechanical Expulsion Deicing System (EMEDS), is a low powered ice protection system that utilizes electronically triggered actuators that work with the composite structure of the aircraft to remove ice from leading edge slats, engine inlet cowls and cockpit windows.

The light system on the aircraft will feature MIL Spec and FAR light systems. Green, red, and white position lights will be placed on the right, left and rear surfaces of the aircraft. In addition, the aircraft will include anti-collision strobe lights on the top and bottom of the center of the fuselage.

VIII. Landing Gear Configuration

Several considerations were made when deciding which landing gear to use in the short take-off and landing aircraft, *Free-Weight*. The landing gear must be robust enough to withstand the short landings on unimproved surfaces as required by the RFP. It must also distribute the load enough to account for the high California Bearing Ratio. Considerations must also be made for the landing gear position in relation to the CG as well as the storage location.

Several aircraft currently in use were researched as a basis for choosing the design of the landing gear for the *Free-Weight*. The C-5 Galaxy features a kneeling landing gear system which allows the cargo floor to be lowered to a height which makes the loading and unloading of the cargo easier. The Galaxy also features two main landing gear pods which house the landing gear, seen in Figure VIII.1.

Figure VIII.1 : C-5 Galaxy
http://www.fas.org/man/dod-101/sys/ac/

Another aircraft, the A400M also has two main landing gear pods which house landing gear that is capable of landing on short, unprepared airfields. The gear has two, six-wheeled main landing gear with long-stroke shock absorbers and three independent lever-type struts per gear. The large number of wheels distributes the load in order for the craft to land on fields with a high CBR. The landing gear can be seen in Figure VIII.2.

Figure VIII.2 A400M
http://airbusmilitary.com/images

VIII.1 Main Gear

The *Free-Weight* will have two, four-wheeled main landing gear with long-stroke shock absorbers, for a total of 8 main landing gear wheels. The lever style landing gear allows the aircraft to be lower to the ground for ease of loading. In addition, they have a lower friction and sensitivity to drag forces. This allows better operation on rough runways. The nose wheel will feature a single strut with dual wheels.

Determining the main landing gear tires is the most important factor when designing the landing gear structure. By calculating the maximum static load for each landing gear, the

dimensions of gear can be chosen from existing tire data. The maximum loading that a tire can sustain, maximum speed that a tire can go, the loaded radius of the tire, and the weights are the factors to consider. With a gross weight of 236,000 lb for the *Free-Weight*, the main gear tire static load is found to be approximately 210,000 lb. The nose gear tire static load is about 26,000 lb. The candidate tires for main landing gears are shown in Table VIII.1 [Reference 28]:

Table VIII.1 Candidate Tire Specs: Main Gear

Outside Diameter (in)	Width (in)	Max Speed (mph)	Max Loading (lbs)	Weight (lbs)
24	8	265	12500	30
34	11	200	18300	77.0
32	8.8	275	23300	75.5
30	8.8	250	21000	57.0
40	14	200	22300	119
40	14	225	27700	130

Comparing the candidate tires, the best configuration yields main landing gear tires with 24 inches of outside diameter and 8.0 inches of width. These are the optimum choice to land on fields with a high CBR.

VIII.2 Nose Landing Gear

Designing nose landing gear takes into account the necessity for ground maneuvering including taxi, take-off roll, landing roll, and steering. With the nose gear tire static load of 26,000 lb, the nose landing gear tires can be determined. The candidate tires for the nose landing gear are shown in Table VIII.2 [Reference 28]:

Table VIII.2 Candidate Tire Specs: Nose Gear

Outside Diameter (in)	Width (in)	Max Speed (mph)	Max Loading (lbs)	Weight (lbs)
20	5.5	185	8750	20.5
22	5.5	160	7100	21.0
24	8.0	265	12500	28.0
25	6.75	275	13000	29.0
27.5	7.5	275	20500	39.0

An optimum tire for the nose landing gear yields tires with the dimensions of 25 inches of outside diameter and 6.75 inches of width.

VIII.3 Shocks

The landing gear must absorb the shocks of landing as well as taxiing. Tires, shock chords or rubbers, air springs, cantilever springs, liquid springs, and oleo-pneumatic struts are the typical devices used for shock absorption in landing gear. Table VIII.3 shows the energy absorption efficiency of these shock absorbers.

Table VIII.3 Energy Absorption Efficiency of Shock Absorbers

Element	Energy Absorption Efficiency (η_s)
Air springs	0.65
Metal springs with oil damping	0.70
Liquid springs	0.85
Oleo-pneumatic	0.80
Cantilever spring	0.50

Using landing weight, vertical touchdown rate, tire energy absorption efficiency, energy absorption efficiency of the shock absorber, number of main gear struts, maximum static load per main gear strut, landing gear load factor, and maximum allowable tire deflection, the required shock absorber length can be calculated from equation 1.

$$s_s = \frac{\left[0.5\left(\frac{W_L}{g}\right) W_t^2 \left\{ \frac{}{W_L N_g} \right\} - n_t s_t \right]}{n_s} \quad (1)$$

Using the maximum static main landing gear load, the required diameter of the shock absorber may be estimated from equation 2.

$$d_s = 0.041 + 0.0025\,(P_m)^{0.5} \quad (2)$$

With the outside diameter of 24 inches, design shock absorber length is calculated as 7.1 ft and the required diameter of the shock absorber is 0.8 ft.

VIII.4 Landing Gear Weight

The weight of the landing gear will affect the overall weight of the aircraft. A typical breakdown of the weight of each part of the landing gear as a percent of the total landing gear weight can be seen in Table VIII.4.

Table VIII.4 Landing Gear Weight Breakdown (% total weight)

Component	Main assembly	Nose assembly
Rolling stock	**32.0**	**2.0**
Wheels	6.0	1.0
Tires	10.0	1.0
Brakes	16.0	0.0
Miscellaneous	0.0	0.0
Structure	**50.0**	**7.0**
Shock strut	32.0	4.0
Braces	12.0	1.0
Fittings	5.0	1.0
Miscellaneous	1.0	1.0
Controls	**7.0**	**2.0**
Total	**89.0**	**11.0**

With the gross weight of the airplane, the landing gear weight can be estimated using equation 3.

$$W_g = 129.1\ (W_{TO}/\ 1000)^{\ 0.66} \qquad (3)$$

Using a gross weight of 236,000 lb, landing gear weight is approximately 4800 lb. By using the previously shown landing gear weight breakdown, the main landing gear weight is found to be about 4300 lb with controls. The shock absorber strut weight is about 1520 lb with two struts.

Cost & Manufacturing

Common military cargo aircraft costs range from approximately 100 to 300 million dollars on average. The *Free-Weight*'s estimated cost falls well within this range at about $165 million per aircraft, assuming a 25 aircraft per year production rate over a duration of 5 years. Costs were estimated using the modified DAPCA IV Cost Model based on constant 2007 dollars. This would create an overall contract cost of $21 billion. Annual operational and maintenance costs, including fuel usage, crew costs for a three-person crew, and scheduled and unscheduled maintenance costs, average approximately $8.1 million per year per aircraft, assuming 1000 flight hours per year.

The considerably low cost of production of this aircraft can be attributed mainly to the extremely low weight of the empty airframe. This was achieved while still avoiding the use of composites where they were not necessary. The low empty weight contributed to keeping many other factors low, including manufacturing hours, tooling hours, and quality control. Another factor that contributed to the very low cost was the use of existing technology for powered lift, such as the EBF's. By utilizing these existing technologies, manufacturing costs are kept to a minimum.

IX. Summary

The *Free-Weight* is an aircraft that has no equivalent in any air force. With the ability to take off and land in under 2500 ft, cruise at over Mach 0.8 at 38,000 ft, all with a 60,000 lb payload, it provides the latest in STOL cargo aircraft and capabilities, while using current day technologies. Utilizing a four engine configuration with Externally Blown Flaps that have been proven in combat situations on the C-17, the aircraft is capable of safe flight even in an engine out scenario.

A key driver for this design was to create a cost effective solution for the United States Military. As such the design avoids complicated and unproven technologies in combat, such as strut braced wings and Upper Surface Blowing. The aircraft itself is a mix of advanced composites and alloys as well as conventional materials to generate the lowest weight aircraft where possible, without adding unnecessary time to manufacturing. Areas where composites are used include the fuselage skin, vertical and horizontal stabilizers and the leading edges while the rest of the airframe is composed of metal alloys.

With a maximum weight of 236,000 lb and the requirement to land on a short rough runway, a durable quad bogie landing gear system was designed to provide reliable operation. To permit a lower landing speed a C_L of 3.8 is achieved using EBF, softening the landing and enabling a landing distance of 2500 ft. The landing gear system itself is podded on the outside of the fuselage to facilitate a lower platform from which to load and unload cargo.

The *Free-Weight* is a new weapon for a new era in warfare. Quickly reaching a combat area to deploy necessary troops, supplies, and even light armor is an essential mission in today's military that now has an aircraft to fulfill that requirement. Future battlefields may not have the large paved runways most cargo aircraft need. With the *Free-Weight*, they are no longer necessary. Any 2500 ft patch of asphalt will do.

Coefficients & Symbols

A_c Spar cross sectional area

C_{Lmax} Maximum wing lift coefficient

$C_{M\alpha}$. Derivative of the pitching moment coefficient with respect to angle of attack

$C_{l\beta}$ Derivative of the rolling moment coefficient with respect to sideslip angle

$C_{n\beta}$ Derivative of the yawing moment coefficient with respect sideslip angle

d_s Diameter of the shock absorber

E Modulus of elasticity

h Spar height

I Area moment of inertia

M Bending moment

N_g Landing gear load factor

N_z Load factor

n_s Number of main gear struts

p Pressure

P_m Maximum static load per main gear strut

r Fuselage radius

s_t Maximum allowable tire deflection

s_s Shock absorber length

t Skin thickness

V Shear force

V_e Equivalent velocity

W_g Weight of landing gear

W_L Landing weight

W_{TO} Take-off weight

w_t Vertical touchdown rate

η_t Tire energy absorption efficiency

η_s Energy absorption efficiency of the shock absorber

σ_u Ultimate strength

References

1. “2024 Aluminum Alloy Sheet and Plate.” Alcoa. http://www.alcoa.com/aerospace/en/products/product.asp?country_id=999&market_id=26&market_cat_id=344&prod_id=595

2. “7075 Aluminum Alloy Plate and Sheet” Alcoa. http://www.alcoa.com/aerospace/en/products/product.asp?country_id=999&market_id=26&market_cat_id=344&prod_id=608

3. “Airbus Builds a Military Airlifter.” Machine Design. http://www.Machinedesign.com/ASP/viewSelectedArticle.asp?strArticleId=57962&strSite=MDSite&catId=0

4. Alcoa Aerospace Product Catalog, 2007. www.alcoa.com

5. “Alloy 2090-T83 Sheet.” Alcoa Mill Products, Inc. http://www.alcoa.com/mill_products/catalog/pdf/alloy2090-t83techsheet.pdf

6. "AN/ALQ-156 (V) Missile Warning System." BAE Systems Brochure "1992" 1-5. 21 Feb 2007 <http://www.eis.na.baesystems.com/brochures/pdfs/01_c18_001.pdf>.

7. Bartolotta , Paul A. and Krause, David L. “Titanium Aluminide Applications In The High Speed Civil Transport.” NASA/TM—1999-209071 1 http://gltrs.grc.nasa.gov/reports/1999/TM-1999-209071.pdf

8. Bird, R. K. , Dicus, D. L., Fridlyander, I. N. and Sandler, V. S. “Aluminum-Lithium Alloy 1441 As A Promising Material For Fuselage.” Translated from *Metallovedenie i Termicheskaya Obrabotka Metallov*, No. 8 (August, 2001): pp. 7 – 10. Electronic.

9. Callister, William D. “Materials Science and Engineering An Introduction.” John Wiley & Sons, Inc, Utah, 2003.

10. Chai, Sonny T., *Landing Gear Integration in Aircraft Conceptual Design*, Virginia Polytechnic Institute and State University, Blacksburg, VA, 1996.

12. Etkin, B and Reid, L. *Dynamics of Flight: Stability and Control, 3rd Ed*. John Wiley and Sons, Inc. 1996.

13. “Engine Placement.” Stanford University. http://adg.stanford.edu/aa241/propulsion/engineplacement.html

14. Ensign, Thomas R. *Performance and Weight Impact of electrical Environmental Control System and More Electric Engine on Citation CJ2*. AIAA 2007-1395.

15. Filippone, Antonio. "Powered Lift Systems." Propulsion Aerodynamics: Powered Lift Systems. http://www.aerodyn.org/HighLift/powered.html

16. Fridlyander, I. N. Khokhlatova, L. B. Kolobnev, N. Rendiks, I. K. and Tempus ,G. "Thermally Stable Aluminum-Lithium Alloy 1424 For Application In Welded Fuselage." Metal Science and Heat Treatment Vol. 44, Nos. 1 – 2, 2002.

17. "Jane's Avionics." Ed. Edwards Downs. Great Britain: Jane, 2004.

18. Lynn, Sean. *Summary Report For An Undergraduate Research Project To Develop Programs For Aircraft Takeoff Analysis In the Preliminary Design* Phase. 1994 http://www.aoe.vt.edu/~mason/Mason_f/TOreport.pdf

19. Krenkel, A.R. and Salzman, *A. Takeoff Performance of Jet-Propelled Conventional and Vectored-Thrust STOL Aircraft*. AIAA Report Vol 5. No. 5. 1968.

20. "Military Analysis Network." 08 Jan 2000. Federation of American Scientists: . 20 Feb 2007 <http://www.fas.org/man/dod-101/sys/ac/equip/index.html>.

21. "Materials." Efunda: Engineering Funamentals. http://www.efunda.com/

22. Matweb: Material Property Data. www.matweb.com

23. MIL-A-8861B. *Military Specification: Airplane Strength and Rigidity Flight Loads.* 18 May 1960. Electronic.

24. Niu, Michael C.Y. *Airframe Structural Design.* Conmilit Press Ltd, 1988. Burbank, California.

25. Roskam, Jan. *Airplane Design Part 1: Preliminary Sizing of Airplanes.* DARcorporation, Lawrence, Kansas. 2003.

26. Roskam, Jan, *Airplane Design Part III:Airplane Design.* DARcorporation, Lawrence, Kansas. 1999

27. Roskam, Jan. *Airplane Design Part IV: Airplane Design.* DARcorporation, Lawrence, Kansas. 2000.

28. Roskam, Jan. *Airplane Design Part V: Airplane Design.* DARcorporation, Lawrence, Kansas. 2003.

29. Roskam, Jan. *Airplane Design Part VI: Airplane Design.* DARcorporation, Lawrence, Kansas. 2004.

30. Roskam, Jan. *Aircraft Design, Part VII*. *Airplane Design.* DARCorportation, Lawrence, Kansas .2004.

31. Sinke, J. "Manufacturing of GLARE Parts and Structures." Applied Composite Materials 10: 293–305, 2003. < http://www.springerlink.com/content/u8166447h23j7111/>

32. Tanner, John A., *Aircraft Landing Gear Systems*, Society of Automotive Engineers, Inc., Warrendale, PA.

33. Vlot, A. and Gunnink, J. W. "Fibre Metal Laminates, an Introduction." Kluwer Academic Publishers, Dordrecht, 2001.

34. Woerden, H. J. Sinke, M. J. And Hooijmeijer, P. A. "Maintenance of Glare Structures and Glare as Riveted or Bonded Repair Material." Applied Composite Materials 10: 307–329, 2003. < www.springerlink.com/index/P0874G1H0173460P.pdf>

35. Wu, Guocai and Yang, J.-M. "The Mechanical Behavior of GLARE Laminates for Aircraft Structures". *Journal of Materials,* January 2005. Electronic.

36. Yechout, Thomas. *Introduction To Aircraft Flight Mechanics*. AIAA, Inc. 2003.

37. Zakharov, V. V. "SOME PROBLEMS OF THE USE OF ALUMINUM-LITHIUM ALLOYS." Metal Science And Heat Treatment Vol. 45, Nos. 1 – 2, 2003